

A Fair Share: Doing the Math on Individual Consumption and Global Warming

Steffen E. Eikenberry, MD, PhD

May, 2018

3.7.3	Hubbert and Peak Oil	57
3.8	An introduction to biomass and biofuels	60
3.8.1	Scalability of bioenergy sources	61
3.8.2	Carbon dynamics	62
3.8.3	Other inputs and emissions	64
3.9	US primary energy consumption	64
4	Emissions from electricity generation	67
4.1	Recent trends in electricity generation	68
4.2	Lifecycle emissions by source	68
4.3	Overall power generation and emissions in eGRID	69
4.4	Marginal and regional emissions	72
4.5	Coal-fired electricity	73
4.5.1	History and current use	73
4.5.2	Coal properties	74
4.5.3	Lifecycle GHG emissions	75
4.5.4	Surface mining, water, and land	76
4.6	Natural gas	77
4.6.1	Overview, the methane leak controversy, and overall GHG emissions	77
4.6.2	A bridge to nowhere? What is the wisdom of a fracking ban?	81
4.6.3	Fracking and water	83
4.6.4	Induced earthquakes	85
4.6.5	A note on natural gas as transportation fuel	85
4.7	Oil	86
4.8	Nuclear energy	86
4.8.1	Nuclear plant operation	86
4.8.2	The fuel cycle	88
4.8.3	Greenhouse gas emissions	90
4.8.4	Safety and health effects contra other power generation	90
4.8.5	Is nuclear power renewable?	90
4.9	Hydropower	91
4.9.1	Greenhouse gas emissions from hydropower reservoirs	92
4.9.2	Reservoir emissions by climate region	92
4.9.3	Other lifecycle emissions	94
4.9.4	eGRID correction	94
4.9.5	Other environmental consequences of dams	94
4.10	Biomass	95
4.10.1	Combustion emissions	97
4.10.2	Overview of regrowth, carbon dynamics, and carbon payoff following harvesting	97
4.10.3	A simple mathematical model for harvesting and biomass GWP	97
4.10.4	eGRID correction	101
4.11	Geothermal	101
4.12	Wind	104
4.12.1	Wind harvesting fundamentals	104
4.12.2	Lifecycle GHG emissions	107
4.12.3	Other externalities	108
4.13	Solar	110
4.13.1	Basics of solar PV	111

4.13.2	Physical fundamentals	111
4.13.3	Emissions factors and energy pay-back time	116
4.14	Limits to renewable energy and energy transition	117
4.14.1	Fundamental resource, land, and material limits to scaling up of renewables	120
4.14.2	Is rooftop solar scalable? Some back of the envelope calculations	122
4.14.3	Some notes on renewable variability and grid integration	122
II	Transportation	125
5	Total per capita transportation emissions	127
	Fundamentals and the personal automobile	129
6.1	How much do Americans drive?	132
6.1.1	American driving patterns	134
6.1.2	Historical fuel economy, and emissions	134
6.2	Basic concepts	136
6.2.1	MPG: city, highway, and combined	136
6.2.2	The hyperbolic relationship between MPG and emissions	137
6.2.3	Operational emissions as a function of MPG and miles driven	138
6.2.4	A note on “fuel consumption” versus “fuel economy”	138
6.3	Petroleum fuels and tailpipe, well-to-pump, and total emissions	141
6.3.1	Tar sands vs. conventional crude and the Keystone XL	142
6.3.2	WTP emissions vary widely by crude oil source	145
6.4	Emissions embodied in vehicle manufacture	145
6.5	Emissions and vehicle weight	149
6.5.1	Fuel consumption and weight, or “size is fuel”	149
6.5.2	Overall emissions	149
6.6	Hybrids, plug-in hybrids, and electric vehicles	153
6.6.1	Overview	153
6.6.2	Emissions embodied in battery manufacture	153
6.6.3	Electric vehicles: understanding MPGe and the MPG_{GWP} concept	155
6.6.4	Marginal emissions and electric vehicles	156
6.6.5	Comparison of major PHEVs, BEVs, HEVs, and ICEVs	158
6.7	The finances of fuel economy	162
6.8	Driving style	164
6.8.1	Overview and effectiveness of general eco-driving techniques	164
6.8.2	Highway speed and fuel economy	165
6.8.3	Idling	165
6.9	MPG_{GWP} equivalent of walking, bicycling, and e-bikes	167
6.9.1	E-bikes	167
6.10	The bottom line	168
7	Physical principles of vehicle travel and alternative drivetrains	169
7.1	“Road-load:” vehicle parameters and driving cycle	169
7.1.1	Overall energy for EPA driving cycles	171
7.1.2	Air conditioning and accessory loads	172
7.1.3	Relative loads: urban driving and cruising	179
7.1.4	Vehicle Mass	179
7.1.5	Aerodynamics	181

Chapter 4

Emissions from electricity generation

For all subsequent sections, it is necessary for us to determine, for various fuels and electricity sources, the *emissions factor* (EF), the mass of CO₂-equivalents produced per unit of fuel combusted or per unit electricity generated. For example, the *direct* EF for coal-fired electricity is roughly 1 kgCO₂e/kWh, meaning for every kWh of electricity generated, greenhouse gases equivalent to 1 kg of CO₂ are produced directly from coal combustion. In addition to combustion emissions, *lifecycle* EFs attempt to incorporate all upstream (e.g. production) and downstream (e.g. waste disposal) processes that also generate emissions, collectively referred to as *indirect* emissions. We must also distinguish between the EF for electricity generated and for electricity delivered, as transmission and distribution losses are not negligible; the latter is relevant for all household operations, except when power is provided by a local generator, e.g. rooftop solar, in which case such losses are near zero.

Another issue to consider is that, while we usually consider the *grid-average* emissions factor for carbon footprinting purposes, small changes in electrical loads, i.e. those acting on the margin, affect *marginal* electricity generation. That is, additional fossil-based generators must be dispatched to meet fluctuating demands, even under electrical grids with very high renewable or nuclear penetrance, and so the marginal EF is usually somewhat greater than the grid-average EF.

The EPA's eGRID database is a comprehensive characterization of nearly all grid-electricity generation in the US, and estimates state, regional, and national electricity-associated emissions using plant-level data. This database is widely used for GHG estimation by both governmental and non-governmental actors. The database considers only emissions at the point of electricity generation, ignoring any upstream or downstream emissions as well as electricity transmission and distribution losses (although these losses are reported). Furthermore, emissions from hydropower, nuclear, wind, solar, geothermal, and biomass are all assumed to be zero. However, there are emissions associated with renewable energy lifecycles, and although these are a tiny fraction of fossil fuel emissions, they are not quite zero. A notable exception to this rule is electricity derived from burning biomass, which likely has an overall carbon footprint comparable to fossil fuels, as I discuss, indignantly, at length.

For a full and honest accounting of electricity-associated emissions, we must account for all lifecycle emissions. In the following sections, I review the literature on lifecycle associated emissions for various electricity sources, and I derive general EFs for all power sources. I also determine crude emissions correction factors (to account for upstream emissions) which I apply to the eGRID database to yield corrected electricity EFs for all regions. I have also attempted to provide a fairly comprehensive understanding of each major power source, controversies surrounding them, and major externalities beyond carbon emissions. I close this chapter with an examination of how scalable renewable technologies are as a replacement for fossil fuels,

primarily in terms of electricity generation, but also as replacements for all global primary energy consumption.

4.1 Recent trends in electricity generation

Coal has been the dominant fuel source for electricity generation since the inception of the grid, and the share of power generated by coal remained above 50% throughout the 1980s and 1990s, until cheap natural gas, largely from unconventional shale sources extracted via hydrofracking (“fracking”), began to significantly displace King Coal, and by 2012, coal had fallen to a 37% share, with NG up to 30% (eGRID), a near doubling over a decade previously; this decline may have stalled however, with coal back to 39% in 2014 (and NG at 28%). The overall effect of this fuel switch on global warming is controversial, due to upstream methane leaks and the effects of cheap fossil fuel on infrastructure and energy use patterns, and the reader is no doubt aware of the controversy surrounding fracking; I explore these issues further in Section 4.6. Despite its deep problems, the displacement of coal by NG has likely been of net climate benefit, although NG remains a carbon intensive fossil fuel source with multiple externalities.

We must understand that the relative demise of coal has little to do with any rise in renewables, and while coal is often referred to almost as a “dead fuel walking,” in the media, it remains the top fuel source for electricity in the US and, especially, globally. Some regions of the US remain almost entirely reliant on coal for electricity. It is also important to understand just how little of the US generating mix comes from non-hydro renewables, i.e. wind (4.4% in 2014), solar (0.4% in 2014), biomass (1.6% in 2014), and geothermal (0.4% in 2014). However, wind and solar have rapidly expanded in just the last few years, and wind power is beginning to become a significant player nationally and especially in certain regions. Of these sources, geothermal is likely only to be developed in a few geologically active regions, and biomass, while renewable, is neither carbon neutral nor scalable (see Section 3.8) and the widespread use of biomass would likely amount to destroying the forest to save it. This leaves wind and solar, both of which truly are low-carbon, scalable technologies that can be deployed on a global scale. The barriers to their universal implementation are primarily social and political, in my view, not technological or environmental (see Section 4.14 for further discussion).

Hydropower (6.1%) and nuclear (19%) are currently by far the most important near-zero carbon electricity sources in the US, but whether they will expand significantly in the future is unclear. American river systems are already extremely fragmented and highly exploited, and thus a major expansion seems unlikely. Nuclear generation is stagnating, and since it relies on limited uranium supplies, it is not actually a renewable energy source. However, under fourth-generation nuclear technologies and breeder reactors, uranium reserves could last millennia, and despite significant emissions associated with plant construction and fuel production, nuclear is a genuinely low-carbon power source (see Section 4.8). Figure 4.1 summarizes recent trends in US electricity generation.

4.2 Lifecycle emissions by source

Figure 4.2 shows the approximate emissions factor for all major power sources, as determined in the following sections, divided into direct and indirect emissions. Error bars indicate the range of what I consider to be reasonably likely maximum and minimums, based on my review of the literature as presented in this chapter. Note that Figure 4.2 shows the EF in terms of $\text{kgCO}_2\text{e/kWh generated}$, while to determine the impact of consuming a single kWh, we need the EF in $\text{kgCO}_2\text{e/kWh delivered}$, which factors in transmission and distribution losses. These

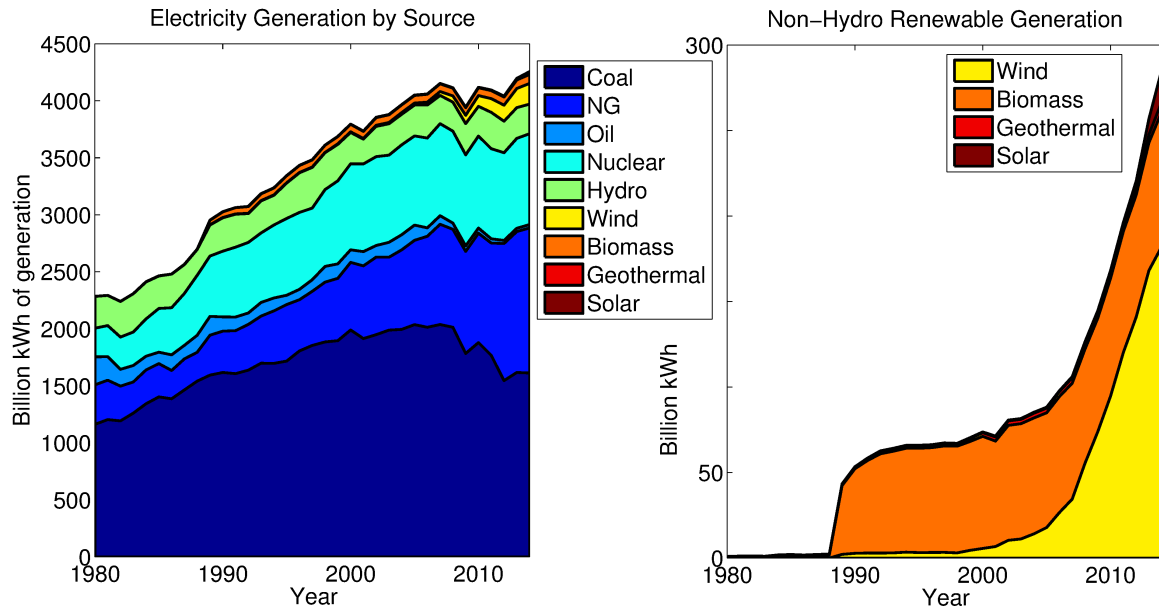


Figure 4.1: Trends in source for US electricity generation from 1980 to 2014 (source: World Bank). The left panel shows that, while coal continues to be the largest single electricity source, it has been partially displaced since about 2000 by cheap unconventional natural gas, while nuclear and hydropower have remained fairly steady. Non-hydro renewables are still little more than a rounding error, but solar, and especially wind, have increased dramatically (in a relative sense) in just the last few years, and wind will likely match or exceed hydro within a few years.

losses are typically around 4–8%, and I take 6.5% as a rough average (the mean T&D loss over the last three eGRID editions). That is, we simply increase the generation EF by 6.5%.

4.3 Overall power generation and emissions in eGRID

About 4.080 billion MWh of electricity were generated (in the US) in 2014, directly generating 2.0914 billion tonnes of CO₂. Coal was responsible for about 74% of this CO₂, with nearly all the balance from natural gas (23%). However, once we account for upstream lifecycle emissions, the US grid probably was responsible for around 2.60 billion MgCO₂e, almost 20% higher than direct emissions alone. In this case, coal and natural gas still account for nearly all emissions, but their respective shares shift to 66% and 27%, with upstream methane leakage accounting for NG’s increased share, and the lifecycle emissions of other electricity sources diluting coal’s share somewhat. Absolute generation and emissions by source are detailed graphically in Figure 4.3.

In terms of kWh generated, I have estimated the overall US grid-average EFs to be 0.5218 kgCO₂/kWh in direct emissions, and 0.6378 kgCO₂e/kWh including all lifecycle emissions. Assuming 6.5% transmission and distribution losses, this translates into direct and lifecycle EFs of 0.558 kgCO₂/kWh and 0.682 kgCO₂e/kWh, in terms of kWh *delivered* (see Figure 4.4). The final number, 0.682 kgCO₂e/kWh, unless otherwise specified, is used throughout this book to determine the carbon footprint of various electricity uses.

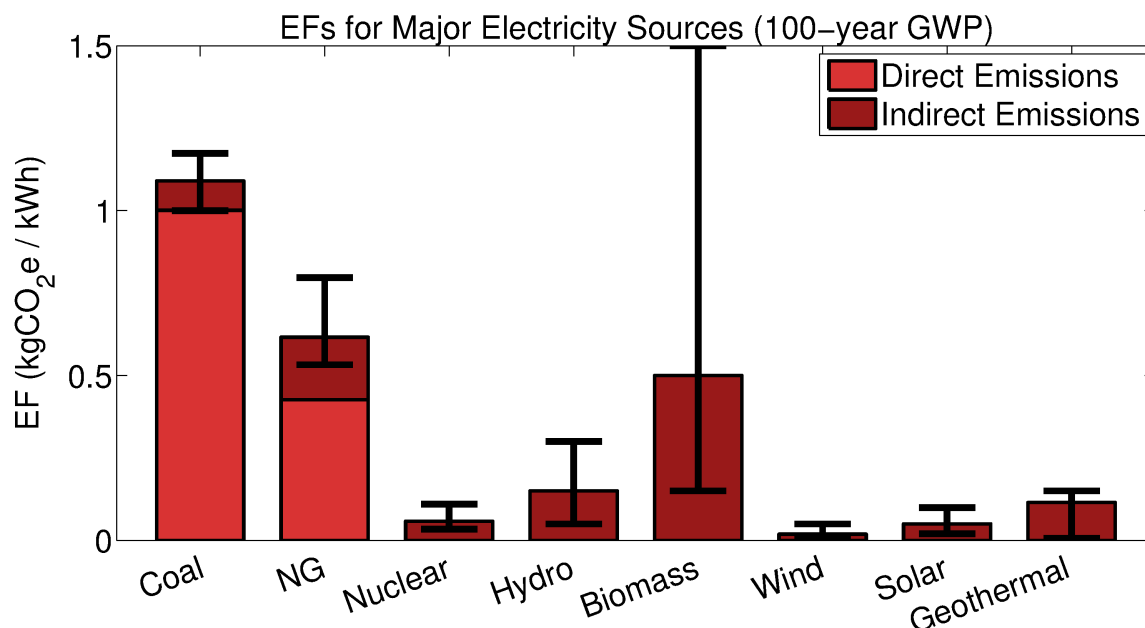


Figure 4.2: Approximate emissions factors for major sources of electricity in the US, over a 100 year time-horizon. Direct and indirect emissions are given, with indirect emissions accounting for 100% of the EF for non-fossil electricity sources; indirect emissions are the source of most uncertainty, and errors bars give my qualitative assessment of the likely maximums and minimums. These EFs are specific to the US grid, and may vary somewhat internationally. For example, tropical hydropower may in some cases be worse than coal, due to very high methane emissions from flooded forests. Out of fossil fuels, natural gas emissions are the most uncertain, varying significantly with the methane leak rate; I take a leak rate of 2.4% as my central estimate. Note that the EF for biomass is highlighted as being extremely uncertain, as most of the impact comes from uncertain effects on forest carbon storage dynamics. Numerically, and for typical power plant thermal efficiencies, my central estimates for upstream emissions are 89 gCO₂e/kWh for coal, 189 gCO₂e/kWh for NG, 58 gCO₂e/kWh for nuclear, 150 gCO₂e/kWh for hydropower, 500 gCO₂e/kWh for biomass, 19 gCO₂e/kWh for wind, 50 gCO₂e/kWh for solar, and 115 gCO₂e/kWh for geothermal power.

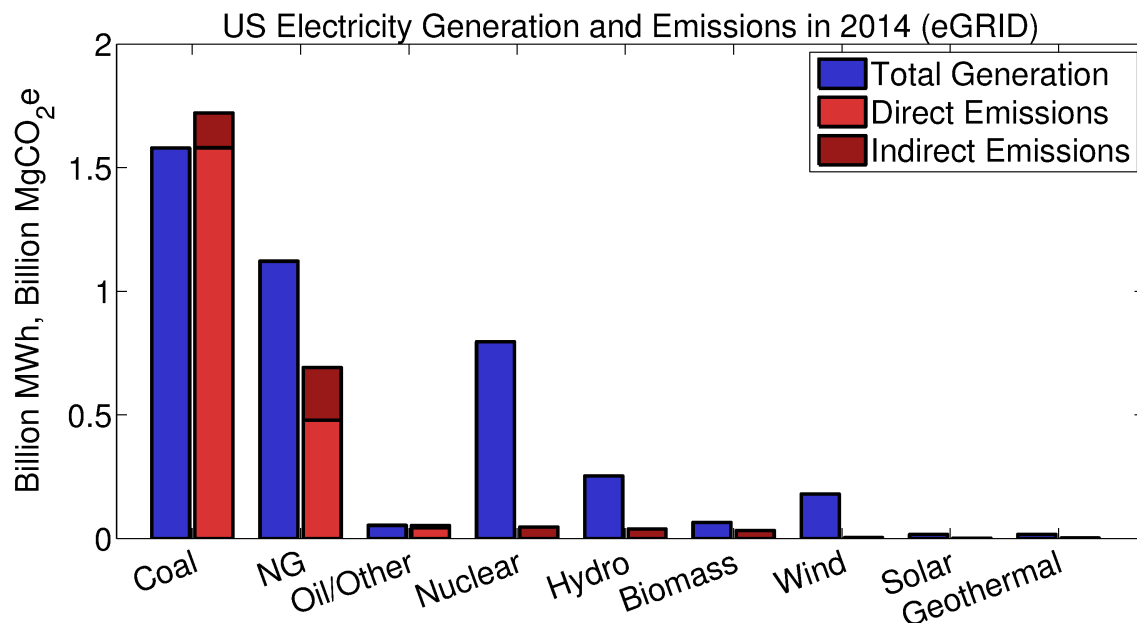


Figure 4.3: Total US electricity generation by source, and total associated (direct and indirect) CO₂e emissions, based on the 2014 eGRID database, and upon the electricity emissions factors derived in the chapter.

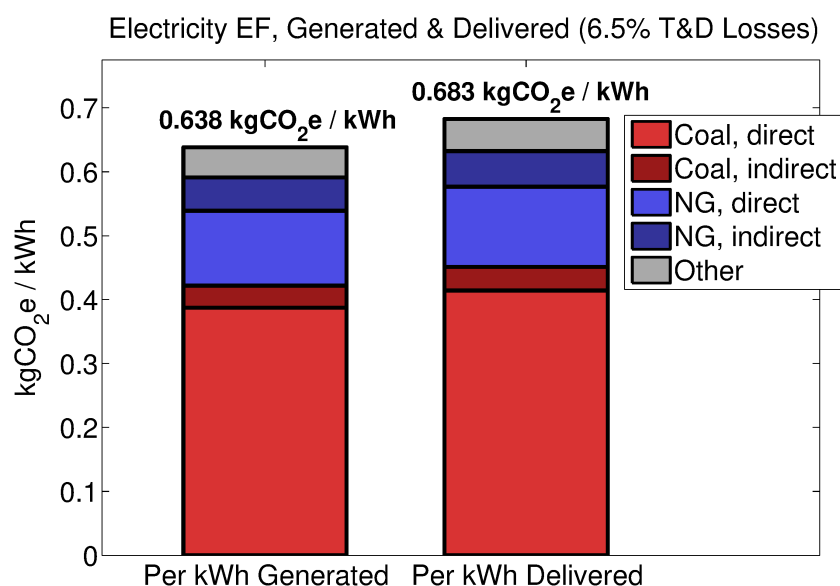


Figure 4.4: Final US grid-average lifecycle emissions factors for electricity generation, either on an as-generated or as-delivered (assuming 6.5% T&D losses) basis. The EFs are derived from the 2014 EPA eGRID database, and from assumed upstream emissions factors as determined in this chapter. The bars show the approximate breakdown of each EF into direct and indirect emissions from coal and natural gas, and all other emissions sources (other minor fossil fuels, and the indirect emissions from all other electricity sources). While other sources account for 33.8% of all generation, they are responsible for only 7.4% of emissions.

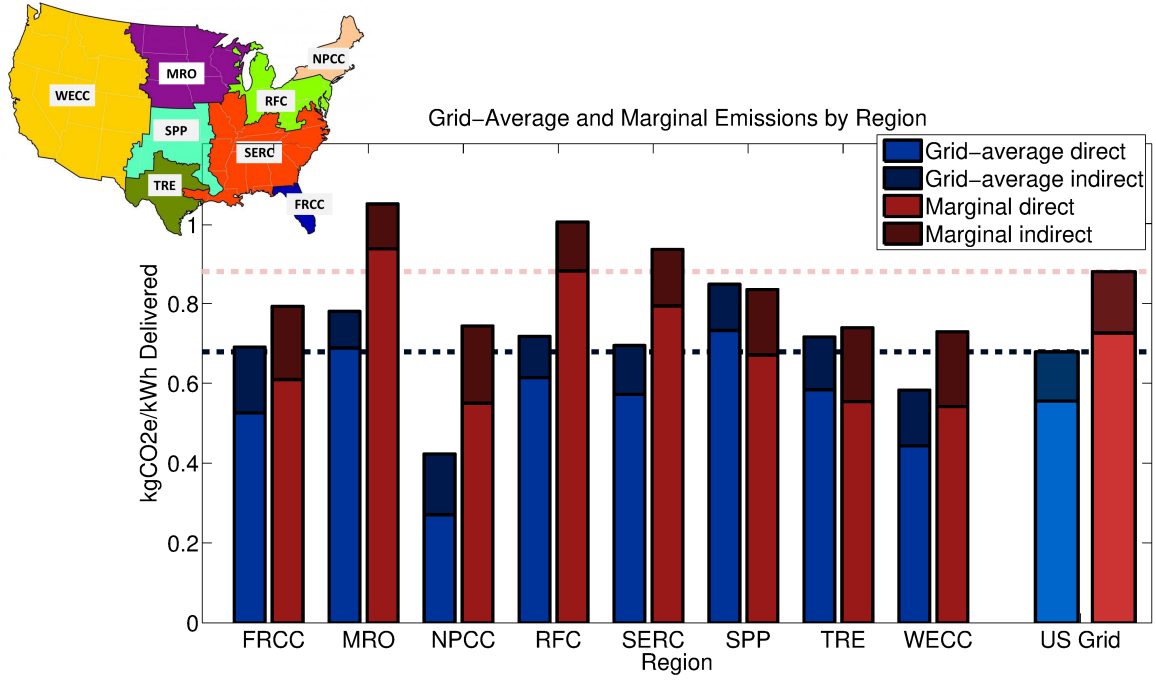


Figure 4.5: Approximate grid-average and marginal emissions rates, in kgCO₂e per kWh *delivered*, i.e. emissions factors include a 6.5% transmission and distribution loss factor, for the eight NERC regions of the continental US, as well as the approximate US averages (0.682 kgCO₂e/kWh and 0.880 kgCO₂e/kWh for grid-average and marginal electricity, respectively). Inset map showing NERC regions is adapted from the EPA’s NERC region map.

4.4 Marginal and regional emissions

Throughout this book, I generally use (my own) derived national grid-average emissions factor (0.682 kgCO₂e/kWh) to measure the impact of electricity consumption. Since regional emissions factors vary quite a bit, the reader must be left to wonder how relevant this single estimate is, but it is not really feasible to provide region-specific estimates for every calculation. Furthermore, since most changes in electricity use represent a *marginal* change, it is worthwhile comparing region-specific marginal emissions factors to the US grid average. As we shall see, the US grid-average EF is a good surrogate for marginal emissions in many regions, but it is an underestimate in regions that are more heavily coal-reliant, especially the midwest.

Siler-Evans and colleagues [74] systematically calculated marginal power generation sources for the eight NERC regions in the continental United States. Marginal power is generated almost entirely by coal and natural gas, with the only exceptions being small amounts of oil-fired generation in Florida and the Northeast. Given the percentage of marginal generation from coal and gas, I calculate an approximate lifecycle marginal emissions factor for each region, as shown in Figure 4.5. I use 1.086 kgCO₂e/kWh for coal, 0.6162 kgCO₂e/kWh for NG (at 42.4% TE, 2.4% upstream leak), and 0.9939 kgCO₂e/kWh for oil-fired generation¹.

These calculations suggest marginal emissions on the order of 0.8798 kgCO₂e/kWh of power delivered (on a lifecycle-basis), almost 30% higher than US grid-average emissions.

¹For oil I use 0.2508 kgCO₂e/kWh(t) combustion emissions (on HHV-basis) and add 0.0573 gCO₂e/kWh(t) of upstream emissions to sum to 0.3081 kgCO₂e/kWh(t). Assuming a 31% TE based, on EIA 2012 data, yields a total EF of 0.9939 kgCO₂e/kWh(e).

4.5 Coal-fired electricity

4.5.1 History and current use

This age has been called the Iron Age...But coal alone can command in sufficient abundance either the iron or the steam; and coal, therefore, commands this age—the Age of Coal. It is the material energy of the country—the universal aid—the factor in everything we do. With coal almost any feat is possible or easy; without it we are thrown back into the laborious poverty of early times.

William Stanley Jevons, The Coal Question (1865)

Coal was known to the ancient Britons and Romans, and it was used intermittently in Europe and Asia since at least the thirteenth and fourteenth centuries for heating, forges, and primitive steam engines [75], but the beginnings of an energy revolution began around 1600, when Britain began to mine and use coal on a larger scale [75, 19]. The first steam engine was patented in 1698 by Thomas Savory, and English coal mining accelerated in the latter 1700s, accompanied by the invention of the efficient Watt Engine. By 1800, 10% of the globe’s commercial energy was provided by coal, as this fossil fuel began to displace wood [75]. Britain led the way, followed by continental Europe, and coal ushered in an age of iron and steam, powering the factories, rail networks, steam-powered fleets, and militaries of the age, in addition to providing heat for domestic use. Coal overcame wood as the world’s chief source of energy by 1880 [75].

It is noteworthy that, from as early as several thousand years B.C.E. until about 1850, the continent of Europe underwent almost continual deforestation, driven by agricultural expansion and the demand for fuel- and construction-wood. With the industrial revolution and the shift to fossil fuels, the forests of Europe stabilized, and have in fact recovered appreciably since their nineteenth century nadir [76, 77].

Coal would itself be displaced by petroleum as the world’s primary energy source by 1950 [75]. With electrification and the rise of oil as the globe’s premier energy source, by the 1970s coal was rarely used residentially and electricity generation had displaced industry as its primary end-use, at least in the US. By 2011, 93% of coal use in the US was for electricity generation, with nearly all the balance industrial (EIA).

From the beginning of widespread electrification post-World War II, coal provided 45–55% of America’s electricity, and indeed, as late as 2010, 45% of all US electricity was coal-generated (eGRID). In the last few years, driven largely by hydraulic fracturing of unconventional sources, natural gas supplies have expanded and displaced some coal generation, yet coal remains the single most important electricity feedstock, holding at 39% of generation in 2014 (World Bank).

There is also marked geographic variation in coal as a generating fuel. In a few states, no coal is used at all: in California < 1% of electrical generation comes from coal, but in much of the mid-west, south, and parts of the south-west, coal clearly remains king. In West Virginia, nearly 96% of all generation is derived from coal, per eGRID. Of course, electricity is widely sold and transmitted across state lines, so state-level generation does not accurately reflect the generation mix for customers in various interconnects (see Section 4.5 for regional emissions factors).

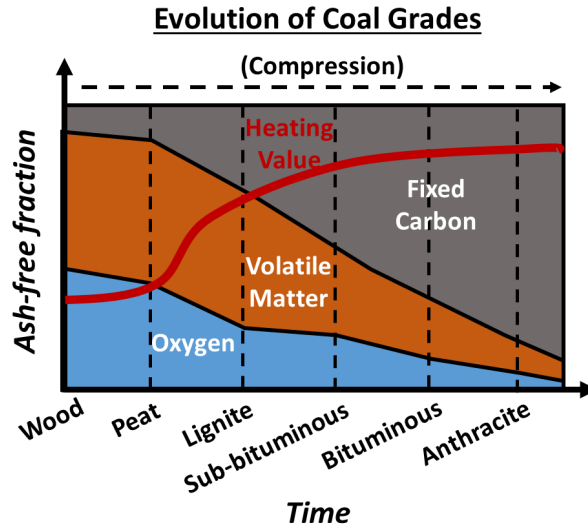


Figure 4.6: Qualitative schematic for the progressive transformation of woody vegetation to peat and, via burial and compression, through various coal grades. With time and pressure, oxygen and volatile matter content falls, leaving highly carbonaceous matter with a relatively high heat content (inset curve). Adapted partly from Figure 3.1 of [54].

Global coal resources are vast, with proven reserves estimated at 1,122 billion tonnes by the EIA (in 2014), while the total resource base may be over fifteen-fold higher [60]. In the US, the EIA reports a demonstrated resource base (DRB) of 433 billion tonnes, with technically recoverable reserves of 231 billion tonnes. While coal extraction and consumption has stagnated in the US, coal use in Asia expanded dramatically in just the last few years. In light of these recent trends, reports of coal’s death may have been greatly exaggerated.

4.5.2 Coal properties

Coal derives, in the main, from ancient marshy forests, where decaying organic matter was buried in boggy, low-oxygen conditions to form peat. As the seas shifted, this peat would be buried under successive waves of ocean sediment. With time, pressure, and heat, water and oxygen are lost, as the peat breaks down into denser and denser carbon-rich material. Thus, we have a progression from wood/vegetation to peat, and then through successive coal grades: lignite, subbituminous, bituminous, and anthracite, as demonstrated in Figure 4.6. The geologically oldest anthracite is highest in carbon, and has the highest heating value of coal grades [54]; by virtue of its high carbon and low hydrogen content it is also the most carbon-intensive coal grade (on a CO_2 per kWh basis) [51]. While coal can be found in every geologic strata, the greatest source is the carboniferous (named, in fact, in reference to its carboniferous coal deposits), an era of vast tropical and semi-tropical swampy forests spreading across the globe’s landmass.

Coal is highly heterogeneous, and a large portion is composed of non-combustible minerals, or “ash.” It is also contaminated by sulfur and mercury, and coal combustion causes serious locoregional air pollution, in addition to its high CO_2 emissions [54].

4.5.3 Lifecycle GHG emissions

- Coal is the foulest burning fossil fuel, and coal plants are relatively inefficient, emitting roughly 1 kgCO₂/kWh of electricity generated.
- Over 90% of coal lifecycle emissions are generated at the point of combustion, with coal mine methane the most significant upstream emissions source. Non-combustion lifecycle emissions sum to about 85 gCO₂e/kWh.

At the point of combustion, coal emits more CO₂ per kWh than any other fossil fuel. The EIA gives combustion emission factors (CEFs) of 0.3348, 0.3280, 0.3177, and 0.3520 kgCO₂/kWh(t) for lignite, sub-bituminous, bituminous, and anthracite coal, respectively, on the basis of thermal energy released, which gives us, assuming the average power plant thermal efficiency (TE) of 32.56% in 2012, emissions factors of 1.0283, 1.0074, 0.9757, and 1.0811 kgCO₂/kWh(e) on the basis of electrical energy generated. Thus, 1 kgCO₂/kWh(e) is an excellent rule of thumb for combustion emissions from coal generation. However, emissions also occur at other stages in the coal lifecycle, and many life-cycle EF estimates for coal-fired electricity have been published for multiple coal plant technologies.

While numerous upstream and downstream processes, including coal transportation, power plant construction, waste management, etc. contribute to coal's carbon footprint, nearly all emissions occur at four major points: (1) coal mine operations, (2) coal mine methane emissions, (3) coal transportation, and (4) direct combustion, with the last accounting for over 90% of the total. Of the processes upstream to combustion, coalbed methane from mines is the most important. A 2012 systematic review and harmonization of coal LCAs by Whitaker and colleagues [79] yielded a median EF of 1,030 gCO₂/kWh (IQR 1,000–1,090 g/kWh), using existing power-plant characteristics. This review estimated that 6% of life-cycle emissions are attributable to methane released during coal mining (point estimate of 63 gCO₂/kWh) and perhaps 2–3% from coal transportation. This work also determined the average CEF for 281 coal-fired plants in 2007 (using eGRID data) to be 970 gCO₂/kWh.

A widely cited study by Jaramillo and colleagues [78] estimated the coal CEF to be 975.0 gCO₂/kWh, and they estimated upstream emissions from coal to range from 39.0 to 78.0 gCO₂/kWh (mean 58.0 gCO₂/kWh), including CO₂ directly emitted from mining operations, methane emissions from coal mines, and the CO₂ emissions arising from coal transport². Using 1997 data as reported by this group, 9.081 million barrels of fuel oil, 1.2 billion cubic feet of gas, 34 million gallons of gasoline, and 49.597 billion kWh of electricity were consumed in coal mining operations, which corresponds to emissions of roughly 36.43 million MgCO₂³. Just shy of 1 billion metric tons of coal were mined in 1997 (9.888×10^8 Mg), and using the reported heat content of 23.193 btu/kg coal, this corresponds to 2,188 billion kWh of electricity, yielding 16.64 gCO₂/kWh for mining operations-related emissions.

Data from the same work [78] also suggests coal mine emissions amounting to 31.10 gCO₂e/kWh, based on the 1997 EPA estimate of 75 million tons CO₂e; correcting from the EPA GWP for methane to IPCC values (i.e. using a GWP of 36 instead of 21) gives 53.31 gCO₂e/kWh. Coal transportation emissions sum to 15.33 gCO₂e/kWh, yielding total upstream emissions of 85.28 gCO₂e/kWh. The grand total of these point estimates is 1,060.28 gCO₂/kWh. However, using the uncorrected mine methane number, we have 1,038.07 gCO₂e/kWh, which corresponds well to the median EF of 1,030 gCO₂/kWh reported by Whitaker et al. [79].

²These EFs are converted from Table 10S into gCO₂/kWh using a thermal efficiency of 32.56%

³Using conversion factors of 0.43 MgCO₂/bbl, 11.146 kgCO₂e/gallon gasoline, 5.26 kgCO₂/lb NG and 0.05 lb/ft³, and 635 gCO₂/kWh for electricity (Jaramillo et al. value [78]).

A later work by the same group [80], using primarily 2010 data, suggests coal production, transportation, and coal mine methane emissions of 6.63 gCO₂e/kWh (95% CI 4.42–7.74), 14.37 gCO₂e/kWh (95% CI 2.21–35.38), and 72.03 gCO₂e/kWh (95% CI 7.58–227.47; corrected from 42.02 gCO₂e/kWh, using methane GWP of 36 vs. 21), respectively, and a CEF of 1,006 gCO₂/kWh. These numbers are derived from the original work assuming a coal plant thermal efficiency of 32.56% (EIA), and give an upstream total of 93.03 gCO₂e/kWh. Yet another study [81] examined lifecycle processes at the level of 364 coal plants in the US, in 2009, and estimated median emissions of 1,060 gCO₂e/kWh generated.

Briefly, we can also obtain a top-down estimate for coal mine methane emissions: the 2014 EPA GHG inventory estimated that 2,631 Gg of methane were emitted by coal mining operations in 2012, while 1,514.04 billion kWh of electricity were generated by coal-fired plants this year. Dividing, we get 62.56 gCO₂e/kWh over a 100-year time-frame (151.18 gCO₂e/kWh using 20-yr GWP), concordant with the studies reviewed above.

In sum, we may reasonably estimate about 7 gCO₂e/kWh, 15 gCO₂e/kWh, and 63 gCO₂e/kWh (151 gCO₂e/kWh using the 20-year GWP) for mining operation, coal transportation, and coal mine methane emissions, respectively, for a total upstream correction of 85 gCO₂e/kWh for coal-fired electricity, over the 100-year horizon (or 173 gCO₂e/kWh on a 20-year basis).

4.5.4 Surface mining, water, and land

As discussed in Section 4.6.3, unconventional gas and oil exploration have uncertain (but almost certainly at least marginally negative) effects on freshwater resources, and can also negatively affect local ecosystems. However, this must be compared to the dramatic, and unquestionably devastating effects that surface coal mining has on streams and ecosystems. Since 1975, coal production in central Appalachia has been increasingly via surface mining, with about two-thirds of coal extracted from surface mines in recent years. A common method is *mountaintop mining with valley fill* (MTM/VF), whereby whole mountaintops are cleared of forest, blasted away, and mined, while nearby valleys and streams are buried with the waste rock [82]. Valley fills can stretch for over a mile, and may be hundreds of meters deep [83]. Such mining is the major driver of land-use change in central Appalachia, and 5% of southern West Virginia had been converted to mine in 2005 [84].

Stream burial and drainage of mine waste clearly degrades regional water quality and deleteriously affects aquatic ecosystems and species. Large tracts of deciduous forest are lost directly to mining, while the forests that remain are highly fragmented. Furthermore, “reclaimed” mining sites support little woody vegetation or biodiversity, and sequester little carbon, even after many decades [83, 82]. The headwater streams buried by valley fills are ecologically sensitive and hydrologically important (as the primary water sources for most rivers), and their burial and contamination affects downstream river networks [84]. Such large-scale altering of the landscape topology also fundamentally alters the regional hydrology [83], and exposure to contaminated water and airborne dust in mined areas appears to negatively affect human health as well [82]. In sum, coal mining probably has regional environmental consequences far worse than any alternative fuel, except possibly tar sands oil (reviewed in Section 6.3.1), including unconventional natural gas extracted via hydraulic fracturing.

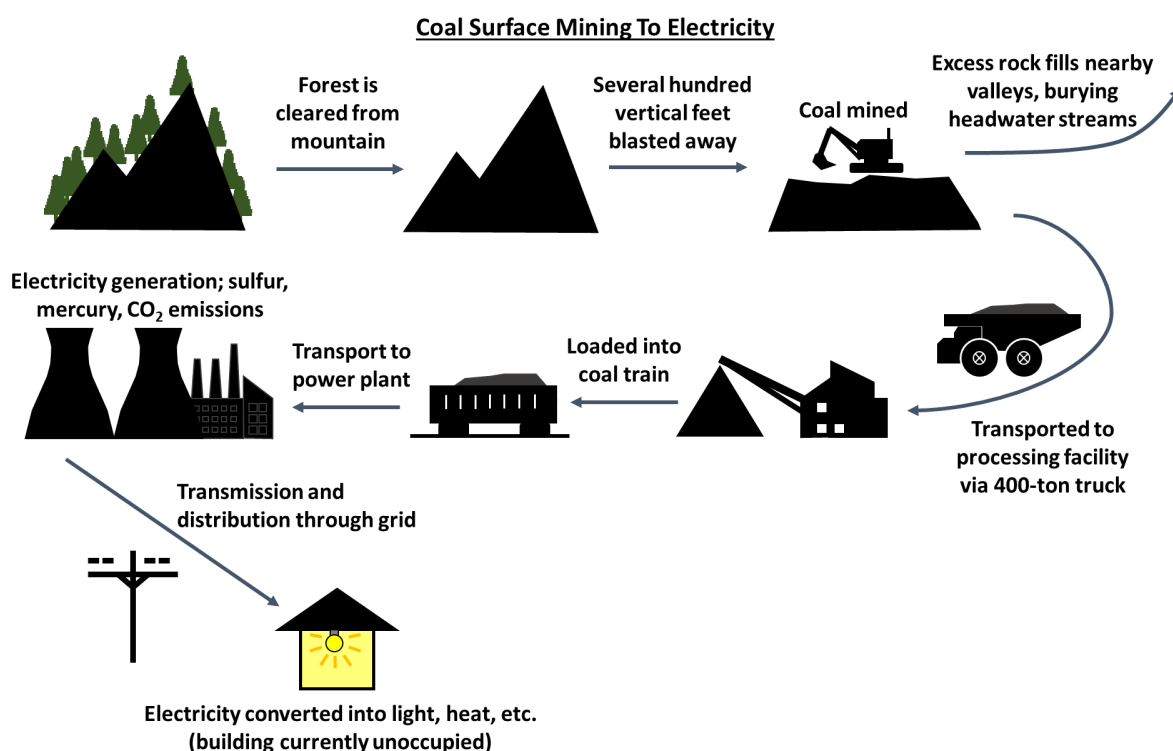


Figure 4.7: Process for extracting coal via mountaintop mining and valley fill, and the downstream generation and delivery of electrical power.

4.6 Natural gas

4.6.1 Overview, the methane leak controversy, and overall GHG emissions

- Natural gas power plants generate only about 40–45% of the emissions of coal plants at the point of combustion, per kWh generated (427 gCO₂/kWh at 42.4% plant efficiency), but high upstream methane leaks, both at the extraction phase (for both conventional and unconventional gas) and distribution phase at least partially undermine this advantage.
- Methane is far more warming than CO₂, but also has a much shorter residence time in the atmosphere. If the leak rate is less than about 3–3.5%, natural gas for electricity is superior to coal over all timeframes, while it is superior at 100 years even for very high leakage (10%).
- The 2015 EPA GHG inventory suggests a leak rate of only about 1.2%, but a variety of observations and modeling studies suggest that methane inventories dramatically underestimate emissions, and a more likely leak range may be 2–4%; I take 2.4% as my central estimate. Including other upstream energy, this suggests upstream emissions on the order of 190 gCO₂e/kWh for typical gas generators.

As reviewed in Section 3.7, natural gas (NG) is formed at great depth, following the burial of organic matter (usually algae, phytoplankton, and other marine organisms) under multiple layers of ocean sediment. Under high heat and pressure, organic matter in low permeability *source* rocks, e.g. black shales, turns to gas and/or oil, from which it migrates to more permeable *reservoir* rocks, forming conventional reservoirs upon encountering a geologic *trap*. Conventional gas supplies, which continue to decline in the US, come from such reservoirs, while unconventional

gas is extracted mainly via horizontal drilling and hydrofracking of the low permeability source rocks themselves (see Figure 4.10 for an illustration of the basic process).

By 2015, according to EIA data, about 70% of US natural gas (NG) production came from unconventional sources, i.e. shale gas, tight gas, and coalbed gas, with shale gas the dominant source. The EIA projects that unconventional gas supplies will continue to increase over the next few decades, while conventional supplies will decline even further. Natural gas has an intrinsically higher energy content than coal, and the carbon content per unit of energy is only 55% of coal's ($0.3259 \text{ kgCO}_2/\text{kWh(t)}$ for coal vs. $0.1809 \text{ kgCO}_2/\text{kWh(t)}$ for NG, using EPA 2013 numbers). Moreover, modern combined cycle gas turbine (CCGT) power plants are much more efficient at converting heat to electricity than older steam generators or (single-cycle) gas turbines, which are comparable to coal-fired steam plants, in terms of efficiency.

EIA data indicates that the average thermal efficiency (TE) of a CCGT in 2012 was 44.8%, and the overall TE of gas generators was 42.4%. Similarly, a report by the California Energy Commission found a 2013 TE of 47.4% for CCGTs deployed in California, with an overall average TE equal to 40.0% for all gas generators. While somewhat inflated thermal efficiencies (TE) of over 50% are often cited for CCGTs in lifecycle analyses favoring gas as an electricity feedstock over coal, it is clear that, as deployed, gas generators are still far more efficient than coal plants, which had an average TE of only 32.5% in 2012 (EIA).

Expanding unconventional production, high energy density, and relatively high thermal efficiencies all have made NG-fired plants an attractive alternative to coal for electricity generation in recent years, and together these factors form the basis for the claim that NG can act as a relatively green “bridge fuel” to a low-carbon future. Indeed, a typical CCGT emits only about $404 \text{ gCO}_2/\text{kWh}$ at the point of combustion, or almost 60% less than the $1,001 \text{ gCO}_2/\text{kWh}$ emitted by a typical coal-fired plant, and converting all coal-fired generation in 2014 (1.58 billion MWh) to CCGT generation could thus save almost 950 million MgCO_2 at the point of generation annually, equivalent to removing about 200 million cars from the road (combustion emissions only), and avoid more emissions than we would by tripling all current wind and solar generation.

Yet, in 2011, a now rather famous analysis by Howarth and colleagues [85] concluded that using NG for electricity, derived from shale gas fracking, is actually *worse* for global warming than burning coal. This analysis had several important flaws, mainly that it compared coal and natural gas on the basis of primary energy, rather than delivered electricity (the main use of coal), and that it failed to account for coal-mine methane emissions. These problems aside, let us examine the fundamental claim, and the subject of much controversy, namely, that the fugitive emissions, or leakage, from natural gas systems increase the global warming potential of NG so much that it is as bad as or worse than coal.

As previously discussed, methane (NG is almost entirely methane) is an extremely potent GHG, especially over the short-term (100- and 20-year GWPs for fossil methane are, including climate-carbon feedbacks, 36 and 87, respectively [7]). Thus, natural gas leakage, which we typically express as a percentage of all gas produced, significantly reduces the relative (and absolute) advantage of NG vs. coal, or if it is great enough, can eliminate it altogether. Estimates for overall leakage, including leaks at both the production and distribution phases, range widely, from around 1–8%. As related in Section 4.6.1, natural gas is superior to coal over all time-frames if the total system leak is less than about 3–3.5%, and it is superior over the 100-year timeframe so long as the leak is less than about 10%, although such a high leak rate still yields extremely potent near-term warming. I now turn my attention to the long-running controversy in establishing this figure.

EPA estimates for the natural gas leak rate have changed dramatically over the years [86], and although EPA reports consistently give very small confidence intervals around the point

estimate, this clearly cannot be valid, given these frequent and dramatic revisions. The still widely cited 2009 EPA estimate of natural gas leak corresponds to about 2.4% of US gas production [86]. The 2015 EPA inventory [10] gives 6.295 million Mg of CH₄ leaking from natural gas systems in 2013, which corresponds to a roughly 1.15% overall leak rate (based on EIA estimated 24,205,523 million cubic feet of NG production in 2013; using density of 0.05 lbs/ft³ this is 598.97 million Mg CH₄).

The EPA estimate of NG leakage from natural gas systems is highly questionable, and it has been heavily criticized. It is largely based on a 1996 study conducted in collaboration with industry, with the 2014 inventory [640] reporting that adjustments were made on the basis of reductions in emissions reported to GasSTAR, a *voluntary* emissions reductions program, and from data on regulations. How these adjustments are made is not transparent. The EPA also relied on a 2012 industry study [641], which claimed much lower methane emissions than previous EPA estimates.

Another paper by O’Sullivan and Paltsev [97] argues that the *actual* methane emissions from bringing a shale gas well online are far less than the *potential* methane emissions. They assume that 70% of such emissions are captured, another 15% flared, and only 15% vented into the atmosphere, citing a 2012 EPA meeting as their source, but there does not seem to anything publicly available to support these numbers. This work also relies on the API/ANGA paper’s [641] assertion that 93% of methane emissions from liquid unloading are captured or flared as its other primary source to support the assertion of high capture/flare rates. A recent study [91] that directly measured onsite well emissions at 190 shale gas sites, in collaboration with well operators, concluded that only 0.42% of gas leaked at the production phase (although additional leakage occurs at downstream transmission and distribution stages, perhaps 0.67% [88]). While these inventories and papers suggest overall leakage on the order of only 1%, almost all other lines of evidence indicate much higher leakage, as discussed now.

Several field studies have directly measured methane fluxes from NG fields, and have consistently measured leak rates far higher than those suggested by the EPA inventory. For example, airborne measurements over the Uintah Basin in Utah [90] suggested leakage of 6.2–11.7% of gas production, although this field is known to be a relatively high emitter. Caulton et al. [87] recently used aircraft to sample a 2,844 km² region in southwestern PA over the Marcellus Shale (by far the most productive play in the US) containing 3,438 wells (57.3% gas, 1.8% oil, 40.8% unknown). In this study, researchers were capable of sampling methane plumes corresponding to individual wells, and they estimated leakage at 2.8–17% of total gas production; a separate bottom-up inventory by the authors estimated 2.09–3.95% leakage. Even more concerning, a method based on remote satellite measurements by Schneising et al. [93] estimated NG leakage of $10.1 \pm 7.3\%$ and $9.1 \pm 6.2\%$ over the Bakken and Eagle Ford formations, respectively, both major shale plays. More modest (but still appreciable) leaks were inferred from 1-day aircraft-based measurements by Peischl et al. [94], who estimated production leakage of 1.0–2.1% over the Haynesville region, 1.0–2.8% from the Fayetteville region, but just 0.18–0.41% over a portion of the northeastern Marcellus Shale.

A comprehensive study by Miller et al. [25] of all anthropogenic methane emissions, using atmospheric methane measurements and weather modeling, estimated that US methane emissions are grossly underestimated by both the EPA and EDGAR, a global methane inventory. Furthermore, they found emission underestimation to be greatest over the south-central US, where there is a great deal of NG and other fossil fuel extraction. They concluded that methane from oil and gas operations is a factor of 4.9 ± 2.6 times too low in the EDGAR inventory and were heavily critical of the EPA’s recent decisions to downgrade its estimates of oil and gas associated emissions.

Conforming with this conclusion, an extensive review by Brandt and colleagues [92] con-

cluded that national inventories consistently underestimate methane emissions at all scales of measurement, a fact that may be partially explained by un-inventoried sources (such as abandoned oil and gas wells), using leak measurements taken on outdated equipment only from cooperating operators, and the strong likelihood that a small number of “superemitters,” that would *necessarily* be underrepresented in inventories, account for a large fraction of total emissions. Various observations also show a 30% increase in US methane emissions from 2002 to 2014 [95], an era corresponding with dramatic expansion in shale gas (and tight oil) extraction.

It is finally important to note that unconventional gas sources do not necessarily suffer from higher fugitive emissions than do conventional wells. For example, a lifecycle analysis by Burnham et al. [88] estimated total methane leakage at 2.75% for conventional gas and 2.01% for unconventional, and Weber and Clavin [89] similarly estimated slightly higher lifecycle emissions for conventional versus shale gas. Still, a focus on shale gas is warranted, since such supplies are dramatically expanding, while conventional gas is nearing its twilight.

A direct comparison to coal

A key paper in the literature is that of Alvarez et al. [86], who compared the integrated warming over all times when using coal versus natural gas for electricity, and when replacing either light-duty or heavy-duty petroleum vehicles with NG-powered alternatives. They famously concluded that NG is better than coal at all time points if the leak rate is under 3.2%.

I perform a similar analysis, incorporating combustion and upstream emissions for both fuels, including coal mine methane emissions. The results are shown in Figure 4.8, and we see that, indeed, at a leak rate of around 3.5%, the short-term warming effect of methane is sufficiently powerful that NG has a stronger integrated warming effect for at least the first few years following combustion. However, only at a leak rate of about 10% or more does warming from NG exceed that of coal out to 100 years, although in this case the 20-year GWP for NG is about twice that of coal. At relatively low, but perhaps the most probable, leak rates, e.g. 2–4%, the 20-year GWP is about 65–95% that of coal, while the 100-year GWP is around 50–65% of coal’s.

Bottom line and eGRID correction

Fugitive emissions from natural gas are uncertain, but likely on the order of several percent (say, plausibly between 1.5 and 5%). I conservatively use the 2.4% figure (based on the EPA’s 2009 GHG inventory) used by Alvarez et al. [86] to derive adjusted emissions factors. I consider this a conservative estimate, despite the fact that the EPA has subsequently reduced their estimate of leakage rates, as the method is not transparent, and the downgrade is at odds with many recent studies that consistently suggest higher methane emissions than those tallied in national inventories. Natural gas for electricity generation almost certainly has a lower climate impact than does coal over the 100-year horizon, and most likely at the 20-year horizon as well, but is still a powerful CO₂e source overall.

Finally, using 1 gC/MJ (i.e. 13.2 gCO₂/kWh) for gas extraction operations [85], and at the 2012 EIA average TE of 42.4%, I calculate 31.13 gCO₂e/kWh for indirect CO₂e emissions from industrial activity associated with well operation. Therefore, for eGRID emissions, I add a crude correction of 158 gCO₂e/kWh + 31 gCO₂e/kWh = 189 gCO₂e/kWh to all gas-fired generating capacity.

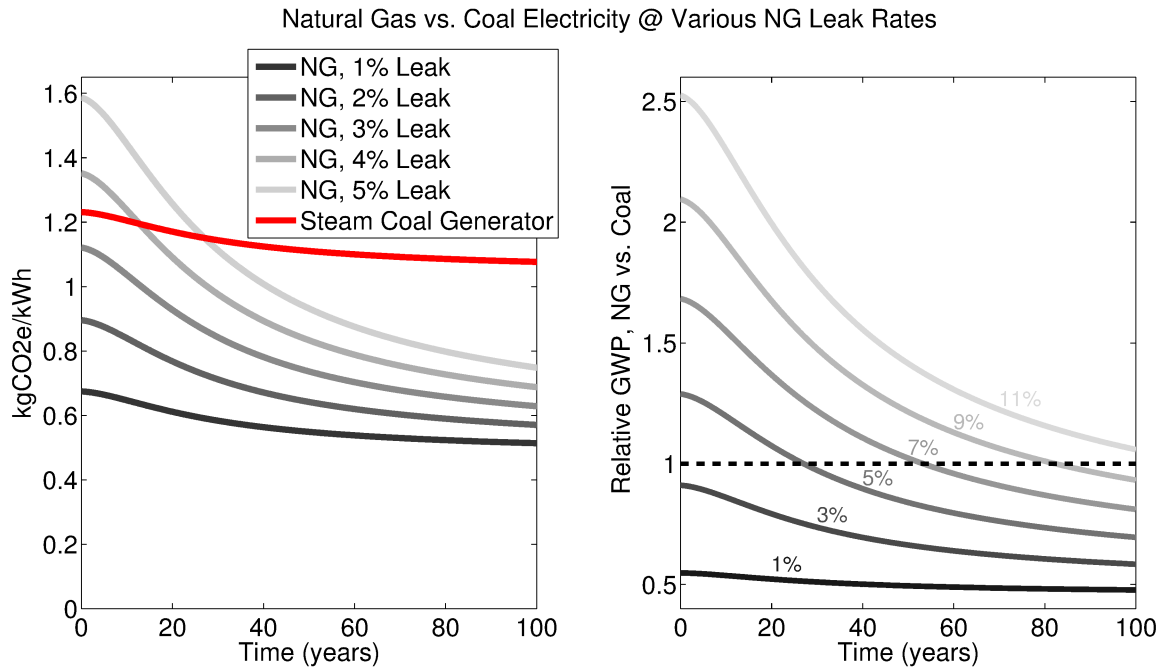


Figure 4.8: Lifecycle CO₂e emissions factors for natural gas and coal-fired electricity, under different NG leak rates (and including likely coal mine methane emissions). The left panel gives the absolute time-dependent kgCO₂e/kWh emissions factors for coal and natural gas at several relatively modest leak rates, while the right panel shows the relative NG to coal GWP over a broader range of NG leak rates.

4.6.2 A bridge to nowhere? What is the wisdom of a fracking ban?

- Compared to restricted supplies, abundant, inexpensive natural gas from fracking is generally projected to displace some coal for electricity generation, but also increase total energy use and compete with renewable and nuclear energy, and have a very minor effect on total greenhouse gas emissions to the year 2050, *in the absence of major energy policy changes*.
- Natural gas from fracking will not reduce carbon emissions, and could increase them, unless it is used as one component of a rational, guided transition to low-carbon energy. However, restricting fracking is also likely to have only a very small benefit at best, if done in a larger policy vacuum.
- Combined with renewable portfolio standards (RPS) (mandated renewable energy targets) abundant natural gas can reduce overall carbon emissions; this is noteworthy as RPSs are widespread at the state level in the US.
- Because of its relatively low CO₂e/kWh (lifecycle) emissions factor, individual use of natural gas is still reasonably advisable for certain domestic applications (such as space heating).

There are two basic competing narratives on the role of natural gas in general, and natural gas derived via fracking from unconventional sources in particular, with respect to the world's energy future, and both largely focus on the role of NG in electricity generation. The first posits that NG is a bridge fuel to a renewable future that will act to displace coal for electricity generation in the short-term, while powering more flexible, load-following power plants that both complement renewables (that is, NG plants can cycle up or down more quickly than coal plants to meet the more variable loads associated with intermittent renewables [98]) and produce

less than half the CO₂ of coal.

The counterargument, essentially that natural gas is a bridge to nowhere, has until recently largely turned on methane leakage from natural gas systems (as reviewed above), with this leakage undermining NG’s relatively low combustion emissions. It is also argued that cheap natural gas, rather than (just) displacing coal, will also outcompete renewables, and furthermore, expanding NG generating capacity and other infrastructure represents infrastructure “lock-in” that will commit energy systems to fossil fuels for decades to come.

As examined at length above, the leakage is highly uncertain, but overall CO₂e emissions, per unit electricity produced, are most likely lower than coal. Further, NG has apparently reduced coal use in the US: the reduction in coal’s share of US electricity generation from 52% in 2000 to 38% in 2014 can be attributed almost entirely to displacement by natural gas. Over the same time period, however, total electrical generation increased 12%, and combined lifecycle emissions from coal and NG electricity generation also ticked *up* about 5%. Thus, the specter of supply-induced demand is raised. It is also important to remember that gas-fired space, water heating, and cooking technologies will also be affected by the availability of NG, and are all generally less carbon-intensive (on a life-cycle basis, and even for relatively high methane leak rates) than the electric alternatives (except heat-pumps for heating). Industrial heating, too, is a major NG end-use affected by availability.

The issue, it would seem, runs much deeper than simply the CO₂e/kWh emissions factor, and we must look at the effect of cheap gas on the whole system-scale carbon emissions, as abundant natural gas is likely to have pervasive effects on world energy markets that could counterproductively increase total energy use (for heating, industrial use, and electricity generation), as well as encourage investment in new NG-based energy infrastructures instead of low-carbon alternatives, undermining (or at least delaying) a transition to low-carbon electricity. Overall, projections [99, 100, 101, 103] of economy-wide energy use under different levels of NG availability have generally concluded that increasing NG supplies *will indeed* slightly increase overall energy use, promote NG over other fuels, primarily coal but, to a lesser extent, nuclear power and renewables, and on balance could either slightly increase [100, 101] or decrease [104, 103] total carbon equivalent emissions, with an increase seeming the more likely outcome.

In one of the more masterly efforts at an integrated prediction, McJeon and colleagues [100] (see also the commentary in [102]) recently evaluated the effect of an “abundant” gas scenario (NG extraction at the likely upper bound of unconventional resources) vs. “conventional” gas scenario (NG extraction limited to conventional supplies) to the year 2050 using five global-scale models used to project energy use, and determined that, in the absence of new political policies, abundant gas would increase total energy use significantly across sectors, but have little effect on total CO₂e emissions. In fact, under most scenarios and models, abundant gas slightly increases global radiative forcing, and while it primarily displaces coal for electricity production, it also decreases renewable generation as well. The major caveat is that these are projections that assume no new energy policies, but importantly, demonstrate that in the unfettered market, fracking and increased exploitation of natural gas will not avert, and may slightly exacerbate, climate change due to market dynamics beyond the CO₂e/kWh metric.

Another very recent modeling effort by Lenox and Kaplan [101], using the EPA MARKAL database (specific to the US energy system), suggested that high availability of NG would slightly increase total electricity production by 2050 and incur higher total carbon emissions compared to a lower NG availability scenario, with this true *across a range* of upstream methane leak rates. Further, the low availability scenario would see greater deployment of renewables.

A general conclusion that can be drawn is that if the market is left to its own devices, increased availability of gas will accelerate the phase-out of coal-fired power, but delay the

adoption of renewables [104], with little overall benefit to the climate. Given this, one policy measure that could synergize to decrease emissions with fracking would be a federal renewable portfolio standard (RPS), i.e. mandated implementation of renewable energy, forcing gas to compete mainly with coal instead of renewables. Even then, however, Shearer et al. [104] projected an RPS would yield only a small difference between high and low gas scenarios (in favor of the high gas scenario), using the EPA MARKAL model. Rather, these authors found that the existence of any carbon reduction policy was vastly more important than the relative availability of NG, with an RPS, carbon tax, or strong emissions reductions requirements all markedly reducing emissions regardless of NG abundance (the RPS scenario was the only one to meaningfully favor high NG).

Note that the conclusions of these analyses are actually quite insensitive to the methane leak rate, with the general conclusion that any climate benefit is equivocal even under very low leak rates [104, 101, 100], while higher leak rates would modestly exacerbate the warming potential of fracking [101, 100].

We can conclude that unconventional natural gas, if it is a bridge to a low-carbon future, is a narrow and treacherous one, but the analyses discussed here suggest this has more to do with the fact that, as an inexpensive fossil fuel, NG will be used on a large scale if available, than it does the controversy over the methane leak rate: the conclusion would be essentially unaltered even without upstream methane leakage. In the absence of a larger policy framework, or widespread voluntary rational use of this resource, shale gas fracking will probably not help the climate and may hurt. It is important to understand, however, that in the absence of either of the former, *with or without* fracking we face climate disaster. It is my conclusion that there would be, from a climate perspective, only a small benefit from a fracking ban, unless it is part of some broader carbon control policy. Under strong renewable mandates, a fracking ban could be slightly counterproductive.

Since the most rational use of NG as a bridge fuel would be as a short-term replacement for coal followed by a rapid phase-out, I offer my speculation that this might best be accomplished by mandated renewable energy targets to force NG to compete primarily with coal (and not renewables), combined with either a carbon tax or carbon cap.

From the individual's perspective, natural gas made abundant by fracking may be rationally used in the short-term for appropriate applications, such as space heating, *so long as one does not take its low price as a license to use it in excess.*

4.6.3 Fracking and water

Perhaps the most contentious public debate surrounding fracking is the one concerning water and this technology: concerns include water used for well development in arid regions and, especially, possible contamination of fresh groundwater supplies, as anyone who watched the 2010 film *Gasland* can attest. However, due to a lack of transparency from industry, the fact that groundwater may suffer methane contamination from both natural and anthropogenic processes, and wide variability in the geologic features of particular shales, it is difficult to reach broad conclusions concerning fracking and water supplies [106]. It is clear that fracking does pose more than a theoretical threat to water supplies, but the overall impact may be small relative to the current scale of oil and gas exploration via fracking; the greatest concern is probably not gas migration in the subsurface, but rather the fate of fracking wastewaters at the surface [108]. It must also be noted that conventional gas and oil exploration can cause similar problems, and conventional gas wells actually generate more wastewater per unit of gas produced than unconventional wells [108].

Fracking may affect freshwater resources via several mechanisms [105]: (1) contamination of shallow freshwater aquifers via migration of stray gas that is mobilized by high pressure

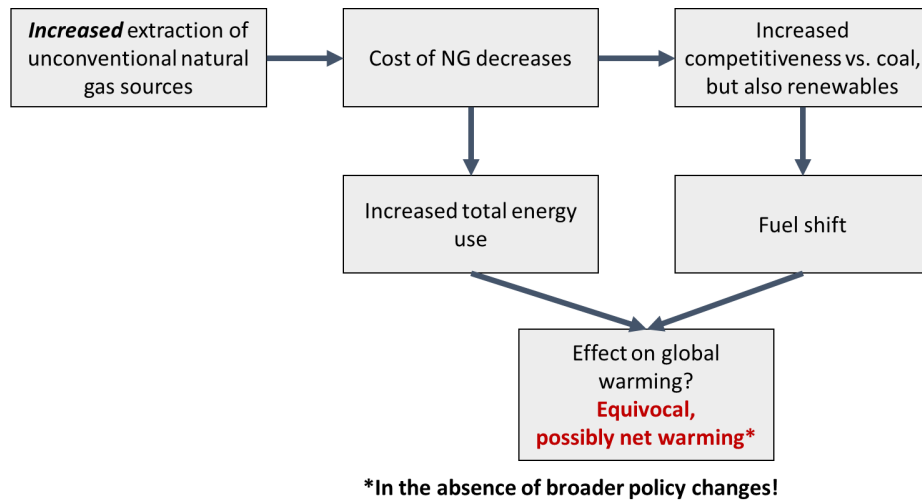


Figure 4.9: Outline for the market-driven outcome of increased extraction of unconventional gas resources, in the absence of any broader policy changes.

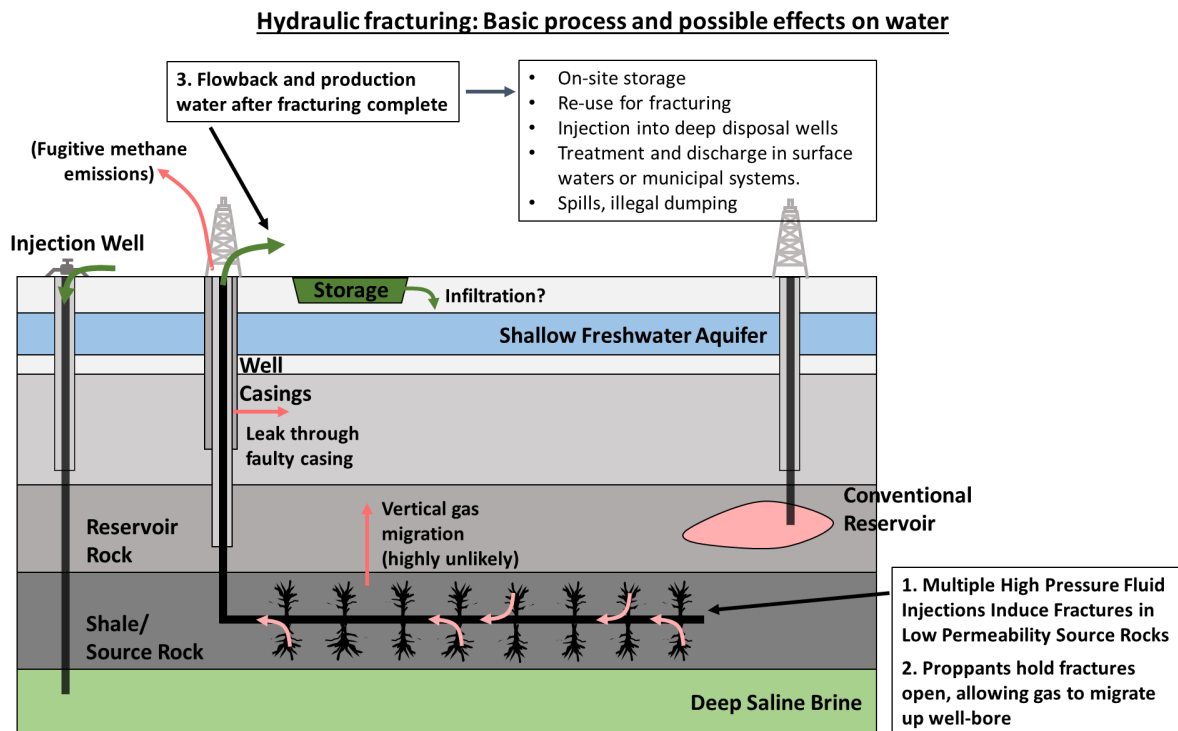


Figure 4.10: Schematic for the basic fracking process, along with some of the possible effects on ground and surface waters.

hydrofracking, or from leaking through faulty well casings, (2) contamination of surface and groundwaters via spills, leaks, or improper disposal of fracking wastewaters, and (3) accumulation of toxic elements near fracking sites. Stress on local water supplies is a fourth mechanism, and while the raw numbers involved in bringing a well online are impressive, on the order of 2–13 millions gallons per unconventional well [105], in the aggregate water used for fracking is but a minuscule fraction of freshwater consumption, accounting for only 0.2% of all water use in Pennsylvania (overlying much of the heavily exploited Marcellus Shale) [108], and less than 0.5% of water use in Texas and several other southwestern states [107]. Still, (sometimes illegal) acute water withdrawals can and have damaged local ecosystems, such as ecologically sensitive creeks [106].

There is evidence that, in the Marcellus Shale underlying northeastern PA, faulty well casings and/or faults induced by fracking have caused some groundwater contamination by methane and possibly by deep saline water as well [105]. Other shales seem less affected, and naturally occurring gas contamination is also common in northeastern Appalachia, so attribution remains controversial [105]. What is less uncertain is that flowback and production fluids (a mixture of water, proppants, other additives, and deep saline groundwater) that return to the surface once a new well is depressurized can contaminate local waters, either when leaching from local storage pools to groundwaters or via accidental, illegal, or even *authorized* discharge into local surface waters or municipal wastewater streams. Dealing with this highly saline wastewater is a major long-term challenge [108]. For now, it is either recycled for new fracturing operations (although this cannot be sustained indefinitely), disposed of in deep injection wells, treated and discharged, or even re-used on roads as a dust suppressant or for de-icing [105]. Some of these issues, and the general fracking process, are illustrated in Figure 4.10.

4.6.4 Induced earthquakes

Several mid-continental areas, most notably Oklahoma, have seen a sharp uptick in seismic activity (defined as frequency of magnitude 3 or greater earthquakes) in the last few years, and this increase is linked to increased oil and gas extraction in these areas. Hydraulic fracturing, *per se*, routinely (and by design) induces microearthquakes, but felt earthquakes from fracking are vanishingly rare in the US [109]. Highly saline wastewater is produced by all oil and gas wells, whether they were fracked or not, and this is routinely disposed of via deep well injection. Injection of water for *enhanced oil recovery* (EOR) can sweep oil towards production wells, and increases well pressure [109]. These latter two activities, wastewater injection and EOR, are more likely to induce felt earthquakes (although this is still extremely rare), and several earthquakes that caused damage have been linked to such activity, such as a 2011 magnitude 5.6 earthquake in OK [110].

Overall, induced seismicity related to well injections, while rather dramatic, has rarely caused felt earthquakes and even more rarely caused damage, and may be mitigated, for example, by well selection and coordinating high-volume injections [110]. Compared to the other externalities associated with the fossil fuel industry, this one seems relatively minor.

4.6.5 A note on natural gas as transportation fuel

While natural gas has been widely promoted as a clean transportation fuel, especially for buses, this notion is, at best, highly exaggerated. For heavy-duty vehicles, the lower efficiency of spark ignition gas engines compared to diesel engines, uncombusted methane escaping the tailpipe, and of course upstream methane leaks, together imply that these vehicles are probably marginally *worse* than the diesel-powered alternatives [86]; for further details see the discussion of natural gas buses in Section 9.1.2.

The lifecycle emissions of NG fueled passenger cars are probably very similar to those of comparable gasoline vehicles. At best, they are perhaps 3–10% less warming over a 100-year time frame, at the cost of increased warming early in time [86]. Gasoline-powered hybrid-electric or electric drivetrains, on the other hand, may generate 40–60% fewer emissions than comparable conventional vehicles.

4.7 Oil

Oil, being far more valuable as a transportation fuel, is increasingly being phased-out as a fuel for electricity generation, and was responsible for only about 0.7% of US electricity generation in 2014. There is little literature directly addressing the upstream emissions from fuel oil for electricity generation, but a 2004 study [111] estimated indirect emissions of 97 gCO₂e/kWh for an oil-fired power plant in Singapore, and a later review by Weisser [112] cites a range of 40–110 gCO₂e/kWh for upstream emissions. Wheel-to-pump emissions for diesel are estimated at 57.3 gCO₂e/kWh(t) by the GREET 1 model (on a HHV basis, see Section 6.3), which is essentially identical to fuel oil. Given an average TE of 31% for oil-fired plants in 2012, this suggests a correction of about 185 kgCO₂e/kWh.

4.8 Nuclear energy

Nuclear power plants generated about 19% of US electricity in 2014, making nuclear, *by far*, the largest source of near-zero carbon energy in the US: hydropower, wind, and solar together accounted for only 11% of 2014 generation. Globally, nuclear power was responsible for 11% of total generation (compared to 17% for hydropower), in 2012 [114]. Nuclear power has, as the reader is no doubt aware, been highly controversial among environmentalists, and it is claimed with some frequency that nuclear is not truly low-carbon, given the emissions associated with uranium mining, enrichment, etc. While nuclear lifecycle carbon emissions are non-zero, a large scientific literature (reviewed in a moment) shows that they are comparable to those of solar power, at around 25–50 gCO₂e/kWh, and calls to phase-out nuclear energy must be viewed in light of these facts. For example, replacing all 2012 nuclear generating capacity with natural gas (at a TE of 42.4%, and 2.4% upstream methane leak) would increase annual US electricity-associated emissions by about 16.9%, or 429.4 million MgCO₂e (and equivalent to 73.3 million cars).

4.8.1 Nuclear plant operation

Let us first briefly review the basic principles of nuclear reactor operation, and the nuclear fuel cycle; for the interested reader, far more detail is available in the technical but readable introduction to nuclear energy by Murray and Holbert [113]. In essence, a nuclear reactor consists of a core, where enriched uranium-235 (U-235) contained in fuel rods undergoes a controlled fission chain reaction, generating heat. A coolant circulates through the core, taking up heat, and then in turn either (1) directly drives a turbine, or (2) passes through a heat exchanger, generating steam in a secondary fluid to drive a turbine and hence generate electricity. Light water reactors (LWRs), the only type currently in commercial operation in the US, use “light” water (i.e. normal water, as opposed to “heavy” water containing deuterium instead of hydrogen) as coolant. When the heated water directly drives the turbine, this is a boiling water reactor (BWR) (about one-third of US nuclear plants), while a system with a heat exchanger is a pressurized water reactor (PWR) (about two-thirds of US nuclear plants).

Note that unused waste heat must be rejected from the coolant water, often with the massive cooling towers frequently mistaken for reactors in the popular imagination. Thus, a nuclear plant is very similar in its broad operation to a coal plant, just with a core burning uranium via fission replacing the coal boiler.

Looking closer at the nuclear reaction, the process is initiated when a free neutron strikes a U-235 atom and is absorbed by the nucleus; the resulting U-236 atom is in an excited state, containing more energy than U-236 in ground-state. This extra energy is released via fission, yielding two fission atoms (which vary widely, but are generally heavy elements), several high-energy (“fast”) free neutrons, and heat, as shown in Figure 4.11. So long as at least one neutron is released per fission event, a chain fission reaction may be sustained.

At this point, we must distinguish between “fast” (high-energy) and “thermal” (slow, low-energy) neutrons, and fissile vs. fissionable material. *Fissile* materials readily undergo fission in response to thermal neutrons, while any nucleotide that undergoes fission is *fissionable*. There is but one naturally occurring fissile isotope, U-235 (there are several “artificial” fissile isotopes, mainly Pu-239 and U-233); all other fission requires fast neutrons, with U-238 and thorium-232 (Th-232) common fissionable fuels. Now, enriched uranium fuel is 3–5% U-235, with the remainder U-238. Fast neutrons released by U-235 fission can be absorbed by U-238 nuclei, and then, via a series of radioactive decay events, give rise to plutonium-239 (Pu-239), which is itself fissile (see Figure 4.11).

Thus, a nuclear reactor can “breed” more fissile material (Pu-239) from the “fertile” U-238. We now have the requisite knowledge to distinguish between *thermal* and *breeder* (or *fast*) reactors. U-235 interacts more readily with thermal neutrons, and a “moderator” can be used to slow the fast neutrons released by U-235 fission, yielding mainly thermal neutrons that go on to interact with U-235 until all is consumed, but leaving most U-238 intact. All LWRs in the US are of the thermal class, use water both as coolant and moderator, and ultimately burn only a small fraction of the fuel uranium (most of the U-235, plus a small amount of converted U-238). Breeder reactors, on the other hand, lack a moderator, and thus rely more on fast neutrons. Since each U-235 fission event releases over two neutrons, on average, there are sufficient neutrons to both breed U-238 to fissile Pu-239, and to sustain the fission chain reaction. The Pu-239 then serves as the source of ongoing fission, until the entire uranium fuel base is consumed. Note that we only refer to a reactor as a breeder if more fissile material is produced than consumed. Thorium, which can be converted to fissile U-233 via absorption of a neutron (similar to the process producing Pu-239 from U-238), represents an alternative fuel base for breeder reactors.

Breeder reactors utilize fuel over 50 times as efficiently as thermal reactors, using nearly all fuel and dramatically cutting waste. Breeder reactors can also burn high-level nuclear waste from thermal reactors as fuel. They have not been widely deployed largely because of higher capital and operating costs compared to thermal reactors, and because of nuclear proliferation concerns (uranium fuel represents only 5% of the cost of nuclear power, and thus there is little financial incentive at present for fuel-efficiency).

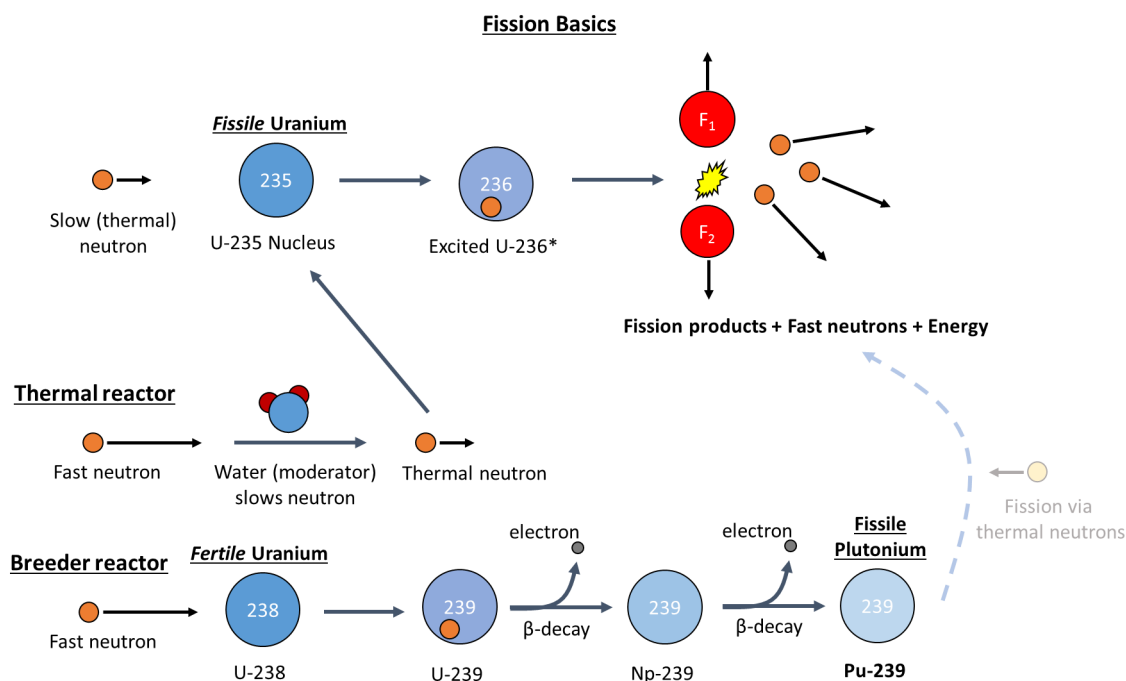


Figure 4.11: Schematic for the basic process of nuclear fission induced in a *fissile* U-235 atom by a thermal (slow) neutron, to yield fission products, fast neutrons, and energy. Fast neutrons can either be slowed by a moderator (water, in most reactors) to induce further U-235 fission (thermal reactors), or may interact with *fertile* U-238 atoms to yield fissile plutonium (breeder reactors).

4.8.2 The fuel cycle

- Uranium from low grade natural ores is milled to U_3O_8 , enriched such that the U-235 isotope concentration increases from 0.7% to 3–5%, and burned in power plants to yield spent fuel consisting of unburned uranium, plutonium, and fission byproducts.
- Reprocessing of spent fuel (as is done in France and several other countries) decreases fresh fuel use by 25% and greatly decreases the amount and radioactivity of the waste.
- The once-through fuel cycle employed in the US stores spent fuel without any recycling of plutonium, yielding waste that remains radioactive for hundreds of millennia.

Uranium, primarily as triuranium octaoxide (U_3O_8), is mined from naturally occurring deposits that vary widely in ore grade, from as little as 0.01% to 15% U_3O_8 , with average ores around 0.1–0.15% U_3O_8 [115, 117]. At processing plants, the raw ore is milled to *yellowcake*: concentrated U_3O_8 . Since only 0.7% of naturally occurring uranium is the U-235 isotope (99.3% U-238), it must be enriched for use in most reactors, to 3–5% U-235, a very energy-intensive process involving conversion of U_3O_8 to gaseous UF_6 , and the major source of greenhouse gas emissions in the fuel cycle. This also leaves large stocks of depleted uranium (U-238) as a byproduct. Fuel fabrication follows, with enriched UF_6 converted to UO_2 , which is assembled into fuel rods. After some months of fission, most of the U-235 has been burned, leaving radioactive fission by-products, large amounts of U-238, and a variety of radioactive plutonium isotopes (and other minor actinides) in the *spent fuel*. The plutonium and minor actinides are

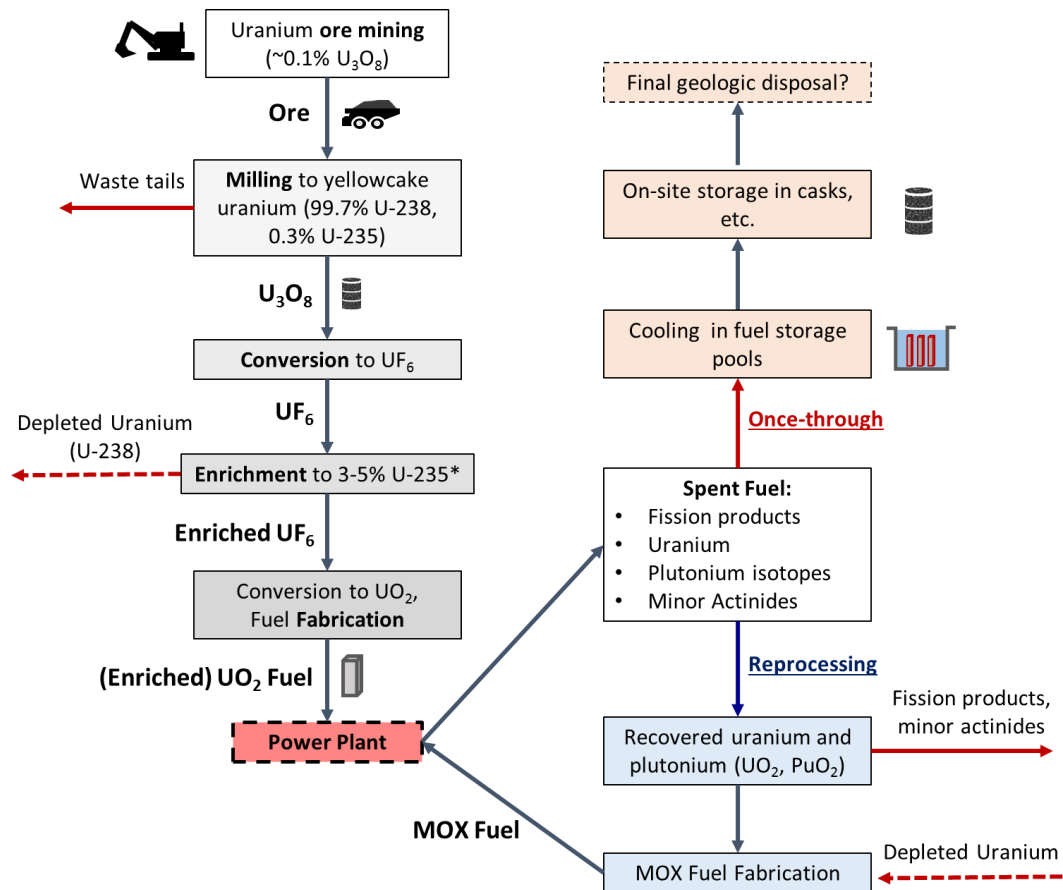


Figure 4.12: Basic uranium fuel cycle for thermal reactors. Spent fuel may either undergo reprocessing and be recycled into the fuel cycle (France, Russia), or disposed in the once-through cycle (USA).

by far the dominant contributors to long-term radiation hazard [113].

The fate of spent fuel varies by country. In the US, the fuel cycle is “once-through,” and, after cooling on-site in water tanks for several years, spent fuel is packaged, stored on-site, and currently awaits final long-term geologic disposal. In many countries, most notably France, spent fuel undergoes reprocessing, where uranium and plutonium are separated from the useless fission products, combined with depleted or slightly enriched uranium to produce mixed-oxide (MOX) fuel (UO_2 - PuO_2), and then mixed with fresh fuel. This reduces fresh fuel requirements by about 25%, reduces the volume of high level waste by about 85%, and, because long-lived plutonium isotopes are removed from the waste, waste radioactivity decreases by several orders of magnitude and largely dissipates within 100 years, as opposed to over 100,000 for once-through waste [116].

Potential fourth generation fast breeder reactors would recycle both plutonium and minor actinides, use fuel vastly more efficiently than thermal plants using either a once-through or plutonium-recycling fuel cycle, and would only generate small amounts of short-lived radioactive waste. Note that this is not a hypothetical technology, but has in fact existed for decades, and multiple operating fast reactors currently exist.

4.8.3 Greenhouse gas emissions

- There is significant variation in the literature, but most estimates for nuclear lifecycle emissions are less than 50 gCO₂e/kWh (amortized over a 30–40 year reactor lifetime), comparable to solar energy.
- Declining uranium ore grade may roughly double lifecycle emissions within 50 years, although this will still represent low-carbon energy.

There are myriad studies attempting to quantify the lifecycle carbon emissions from nuclear power, as reviewed by various authors [120, 117, 118, 119], and, for LWRs, estimates range from practically zero gCO₂e/kWh to over 200 gCO₂e/kWh; relatively recent reviews give mean estimates of 60 [120]; 66 [117]; 8, 58, or 110 gCO₂e/kWh depending on assessment method [118]; and a median of 12 gCO₂e/kWh in the most recent review [119]. The distribution of estimates is highly skewed to the right, with most studies estimating lifecycle emissions under 50 gCO₂e/kWh [117, 121]. Therefore, the overall mean may overstate true emissions.

Broadly speaking, emissions sources are (1) the front-end fuel cycle (uranium mining, milling, enrichment, and fuel fabrication), (2) power plant construction, (3) plant operation and maintenance, (4) eventual plant decommissioning after 30–40 years (sometimes including mine site clean-up and rehabilitation), and (5) the back-end fuel cycle (storage and disposal for the once-through fuel cycle). All phases require significant energy, and power plant construction requires on the order of several hundred thousands tonnes of carbon-intensive materials (e.g. over 150,000 tonnes of concrete) [117], but the comparative impact of each category varies significantly by source [117, 118].

One aspect worthy of special consideration is the influence of uranium ore grade on emissions, as average ore grade is likely to decline in the future [121]. Warner and Heath [119] estimated that lifecycle emissions could increase by 55 to 220%, while a more recent study by Norgate et al. [121] projected average emissions to increase from 34 gCO₂e/kWh to 60 gCO₂e/kWh over the next 50 years, assuming a concomitant decline in average ore grade from 0.15% to 0.01% U₃O₈. For my corrected eGRID emissions estimates, I have somewhat conservatively chosen 58 gCO₂e/kWh (middle estimate from [118]) as my correction for nuclear power.

4.8.4 Safety and health effects contra other power generation

While major nuclear disasters and waste toxicity are rightfully of concern, out of all major electricity sources, nuclear is associated with the *fewest* excess deaths per kWh of electricity generated [122], whereas coal, primarily via increased cardiac and respiratory mortality related to particulate emissions, causes several tens of thousands of deaths yearly in the US [124] and several hundred thousand deaths worldwide. On a per kWh basis, coal causes perhaps 500–1,500 times more deaths than nuclear [122]. Furthermore, nuclear power has likely acted to significantly displace coal as a power source historically, and on this basis Kharecha and Hansen [123] estimated that nuclear power has saved 1.84 million lives since its inception.

4.8.5 Is nuclear power renewable?

Uranium is a finite resource, and therefore nuclear power, while low-carbon, is not renewable. Under current rates of uranium use (almost universally using the once-through fuel-cycle) known and inferred uranium resources will last around 200 years. Once we take into account projected growth in demand, see e.g. EIA projections as discussed by Mudd [115], or assuming annualized

growth of 1.9% [121], without improvements in efficiency reserves may last less than 100 years, and uranium supplies would necessarily peak before exhaustion of the fuel base. However, reprocessing of nuclear waste can reduce overall fuel requirements by 25% [116]. Breeder reactors, which have not been widely deployed largely because uranium proved to be far more abundant than initially expected, use but 1% the fuel consumed by current thermal reactors. Seawater represents a nearly infinite uranium source, although it is not currently economical to extract it, and thorium can also serve as a nuclear fuel, with the thorium cycle offering multiple potential advantages over uranium.

Since breeder and thorium reactors both currently exist, and it is economics (and proliferation concerns, in the case of breeder reactors) rather than technological barriers that have prevented their widespread adoption, nuclear power *could* act as a quasi-renewable technology, supplying power for many thousands of years (and possibly millions, if uranium could be extracted from seawater or other unconventional sources at large-scales).

4.9 Hydropower

- Hydropower is a low-carbon energy source overall, but has higher lifecycle emissions than other low-carbon energy sources, including solar, wind, and nuclear.
- The decay of flooded vegetation in reservoirs leads to significant carbon dioxide and methane emissions, and hydropower in tropical regions may actually be much worse than coal in terms of lifecycle CO₂e emissions.
- Large-scale damming of the world's river systems has other serious consequences for biodiversity, water quality, and the global hydrologic cycle.

Large-scale hydropower generated about 6.1% of all US electricity in 2014, making it the second-most important source of low-carbon energy, after nuclear. Globally, however, hydropower is more significant, at 17% of generation [114], and while there was little new installed capacity in the last several decades, there has been a recent rush to expand hydropower in emerging economies, especially in Amazonian regions, China, and southeast Asia, with a focus on mega-dams, and thus global hydropower capacity is projected to increase 73% in the next 10–20 years [130]. This is extremely controversial, as large-scale damming of over half the world's major river basins already profoundly affects the global hydrologic cycle with severe adverse effects on riverine and terrestrial ecosystems, biodiversity, and water quality. Dam mega-projects also displace large human populations, and catastrophic dam failures have resulted in thousands of deaths [125]. Finally, since tropical hydropower generates significant CO₂e emissions, it is unclear what benefit, if any, this hydropower boom will have for the climate [126, 127].

While there are no direct GHG emissions⁴ associated with hydropower, flooding of vast areas and subsequent anaerobic decay of vegetable matter is a significant source of methane and CO₂, especially in tropical regions (where much new hydropower development is slated to occur), and it is likely that the global warming effect of at least some tropical hydropower is worse, and perhaps far worse, than coal [126], although hydropower in the temperate and boreal regions of North America is more benign. Other more minor lifecycle sources of carbon include dam construction, which requires large amounts of cement and other materials, and dam decommissioning at the end of life, which may release carbon from reservoir sediments.

⁴Although we could arguably consider the degassing of CO₂ and CH₄ from water passing through dam turbines as a direct emission, this is itself a consequence of anaerobic decay in the dam reservoir.

4.9.1 Greenhouse gas emissions from hydropower reservoirs

Dams and the resulting reservoirs alter carbon dynamics in several ways. Most importantly, dams flood wide expanses of land, submerging large amounts of vegetation (especially in former forests), and for the first 10–15 years after flooding, great quantities of CH_4 and CO_2 are released as this labile carbon pool degrades [129]. Detailed measurements of several individual reservoirs have shown these early emissions to decrease until a steady-state is reached, with further CO_2/CH_4 emissions coming from new biomass either growing in the reservoir or entering from outside (e.g. via rivers or runoff). The deep water of reservoirs is often anoxic, promoting anaerobic degradation of organic matter that favors methane production.

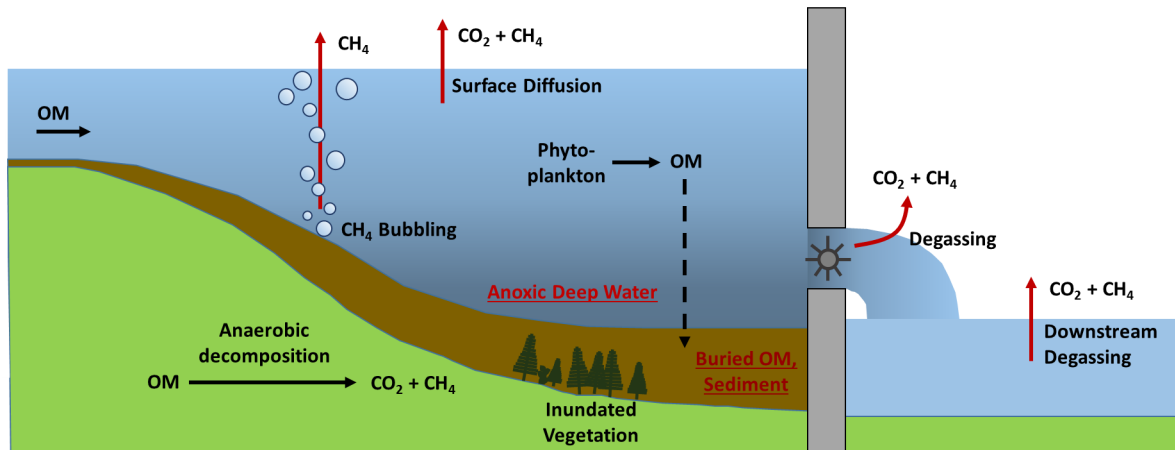
There are several pathways for greenhouse gas (CH_4 and CO_2) release from reservoirs. Most simply, these gases diffuse from the reservoir surface at the water-air interface. Second, bubbling is a major source of methane (methane has very low solubility in water, hence the formation of bubbles), where CH_4 produced in deep anaerobic sediments bubbles to the surface. Third, deep water passes through turbines near the base of dams. Since this deep water is cold and under high pressure, it can be supersaturated with respect to CH_4 and CO_2 , and thus we have degassing from the turbulent flow through turbines and further on downstream. The latter two sources are significant, but have not been included in many studies [129], and thus GHG flux from reservoirs has probably been systematically underestimated. Finally, a generally neglected source of carbon emissions is the decomposition of above-water deadwood in flooded reservoirs, which Abril et al. [134] found to contribute about one-third of all carbon emissions in two tropical reservoirs. Figure 4.13 summarizes these GHG sources.

Reservoirs also alter global carbon flows, as significant amounts of organic matter enter freshwater from land, perhaps 1.9 PgC, and of this, Cole et al. [128] estimate that 0.23 PgC is buried in sediment (mainly in man-made reservoirs), 0.75 PgC is oxidized to CO_2 , while 0.9 PgC finds its way to the ocean, where 25% may enter the deep ocean and be lost to the short-term carbon cycle [129]. Burial in reservoir sediment represents a carbon sink attributable to dams, although this may in turn reduce downstream sedimentation and carbon storage in the deep ocean [129], and the anoxic carbon sediments can also evolve to methane. Furthermore, sediment build-up in reservoirs eventually necessitates dredging or dam removal, at which point carbon contained in sediment may be released as CO_2 and CH_4 in amounts significant even when amortized over a 100-year dam lifetime [137].

We must further distinguish between gross and net emissions from reservoirs. *Gross* emissions are those discussed above, the CO_2 and CH_4 released from various points in the reservoir. *Net* emissions, on the other hand, are the net emissions that result from commissioning a hydroelectric dam after accounting for the previous carbon source/sink activity of the flooded land and, ideally, all downstream effects on the carbon cycle. For example, forests are generally considered a carbon sink, and so flooding of this sink increases net emissions independently of gross reservoir emissions.

4.9.2 Reservoir emissions by climate region

Several recent reviews [131, 129] have concluded that equatorial and, especially, tropical, reservoirs have far higher GHG emissions than temperate or boreal reservoirs. This is likely due to warmer water temperatures, increased biomass, and a tendency for tropical reservoirs to have a deep anoxic zone [131, 129]. From 150 literature estimates, Hertwich [129] determined globally averaged emissions factors of 85 gCO_2/kWh and 3 gCH_4/kWh , equating to 187 $\text{kgCO}_2\text{e}/\text{kWh}$. Assuming that power density (i.e. kWh generated per m^2 of reservoir) is similar across climate regions, from Table 2 of this work I calculate emissions of 233, 67, and 309 $\text{gCO}_2\text{e}/\text{kWh}$ for boreal, temperate, and tropical regions, respectively. However, because many works did not



1. Organic matter (OM) from inundated vegetation, upstream river, and local phytoplankton is buried in anoxic sediments, leading to anaerobic decomposition and CO₂ and CH₄.
2. GHGs released via CH₄ bubbling, surface diffusion, turbine degassing, and further downstream degassing.
3. GHG emissions in first decade of reservoir creation dominated by decomposition of inundated vegetation.
4. Subsequent steady-state emissions from ongoing OM transport and reservoir production.

Figure 4.13: Schematic for major pathways by which CO₂ and CH₄ are emitted from hydropower reservoirs. Organic matter buried in deep, anoxic waters decomposes anaerobically, yielding CO₂ and CH₄, which may diffuse into the atmosphere across the water-air interface. Methane has extremely low solubility in water, and so much is released by bubbling. Further, these gases may dissolve into water at depth (under cold, high pressure conditions) but then de-gas after passing through turbines, both at the turbine and further on downstream.

measure methane bubbling and downstream bubbling/diffusion—a very significant methane source in tropical reservoirs [133]—is commonly neglected, these are assuredly underestimates and could easily be twofold higher. Further, above-water biomass decay has only been considered (to my knowledge) for two tropical dams (Petit Saut and Balbina [134]). It is therefore worthwhile to examine some particular studies more closely.

While overall, measurements are available for only a tiny fraction of equatorial and tropical dams, and these vary in how comprehensive they are, based on what data there is, many tropical hydroelectric reservoirs appear to be comparable or worse than coal (see, for example, Figure 4 of [132] and the discussion in [129]), with the few tropical dams for which detailed measurements are available showing very high CO₂e emissions indeed. The Petit Saut dam, located in French Guiana, was commissioned in 1994, and comprehensive field measurements [133, 134] over the subsequent decade suggest CO₂e emissions of, at a minimum, 0.8 kgCO₂e/kWh amortized over 100 years [134] (this estimate assumes CO₂e emissions fall ten-fold and remain constant after 10 years, which is almost certainly too conservative). Fearnside [126] estimated emissions of 6.683 kgCO₂e/kWh over the first twenty years of operation, for Petit Saut, implying an absolute minimum of 1.337 kgCO₂e/kWh over 100 years. The Balbina reservoir in Amazonian Brazil, commissioned in 1987, is even worse, emitting at least 2.5 kgCO₂e/kWh amortized over 100 years [134], and much more over the near term, with Hertwich giving 11.9 kgCO₂e/kWh [129].

It should be noted that the Petit Saut and Balbina reservoirs have a low energy density, in terms of kWh generated per m² reservoir area. Since GHG emissions are roughly proportional to the reservoir area, it follows mechanistically that higher energy density reservoirs should have lower emissions per power output; this is strongly supported by existing data [129]. A comprehensive simulation study of possible GHG emissions for 18 new and planned Brazilian hydroelectric reservoirs [136] suggested great uncertainty and an extremely wide range in emis-

sions factors, with some high energy density projects showing low emissions, but some others possibly comparable to natural gas or coal plants.

Temperate and boreal reservoirs are much less harmful. For example, a detailed seven-year study [135] of a new boreal hydroelectric reservoir in northern Quebec, Canada gave *net* reservoir emissions of about 158 kgCO₂e/kWh, when projected over a 100-year dam lifetime.

4.9.3 Other lifecycle emissions

Dam construction is a very minor source of lifecycle emissions, perhaps about 4 gCO₂e/kWh (see [126] and the references reviewed therein). More significant, and as already mentioned, sediment build-up traps large amounts of organic matter, which eventually can be exposed and evolve to CO₂ and CH₄ with reservoir dredging or decommissioning. Pacca [137] estimated the GWP of sediment carbon mineralization, across six US reservoirs, to be 35–104 gCO₂e/kWh if 3% of sediment carbon mineralizes, and 128–380 gCO₂e/kWh if 11% mineralizes.

4.9.4 eGRID correction

The review by Hertwich [129] suggests reservoir emissions of 67 and 233 gCO₂e/kWh for temperate and boreal hydroelectric reserves, respectively, but based on many studies that likely systematically underestimated emissions. Teodoru et al. [135] suggested net emissions of 158 gCO₂e/kWh for a new boreal reserve, and dam construction and decommissioning likely add at least 40 gCO₂e/kWh. Therefore, I adjust eGRID hydroelectric emissions upward by 150 gCO₂e/kWh, which I consider conservative.

4.9.5 Other environmental consequences of dams

- Extensive damming of a majority of the world’s major river systems is a major component of global-scale alteration of the hydrologic cycle, with adverse consequences for many ecosystems.
- Damming supports water withdrawals for agriculture and other human needs, and so adverse consequences are only partially attributable to hydroelectricity.

Dams are ubiquitous throughout the world’s river systems: there are over 45,000 dams higher than 15 meters (49.2 ft) [142] and over 800,000 smaller dams [141], which collectively act to obstruct about two-thirds of the freshwater flowing to the ocean [141] and fragment half to two-thirds of the world’s major river systems [142]. Essentially all major river systems in the continental US are heavily fragmented by damming [142]. This represents a fundamental alteration of the hydrologic cycle, with myriad consequences for both aquatic and terrestrial ecosystems [140]. Dams are constructed not just to provide electricity, but to control flooding, river flow, and divert large amounts of water for irrigation and other uses, and so the ecological consequences of dams are not attributable to hydroelectricity alone. In particular, humanity appropriates about half of all available freshwater via its various waterworks, overwhelmingly for agricultural irrigation [140]. Nevertheless, the focus of many new giant dams is on electricity generation.

The most obvious consequence of damming is the inundation of large areas of upstream land and wholesale destruction of the associated ecosystems. River fragmentation by dams blocks migration and dispersal of many species, and has caused the extinction of many fish populations and even species [142]. Water withdrawal adds further stress, with withdrawals

from many rivers so extreme that they no longer even reach the ocean. The reservoirs that result from damming also lose far more water to evaporation than do free running rivers [141].

Siltation of reservoirs reduces silt transport downstream, which in turn can increase erosion and alter coastlines that previously depended on silt influx. Dams chiefly act to reduce variability in river flow and eliminate flooding, whereas the natural cycle is typically one of annual flooding of a downstream floodplain, bringing nutrient rich sediment and water to a wide region: ancient Egyptian agricultural was famously dependent upon the annual flooding of the Nile for fertilization, a cycle that has now ceased. Floodplain ecosystems are usually highly adapted to this annual cycle, and its disruption has broadly negative effects [141].

4.10 Biomass

- Harvesting woody forest mass for electricity is not carbon neutral over a timescale of decades to centuries, and moreover, integrating the warming effect of harvesting on forest carbon dynamics over 100 years shows that emissions factors for live tree harvesting may range over an order of magnitude, from perhaps 0.2 kgCO₂e/kWh to 2.0 kgCO₂e/kWh (in terms of electricity generated), with the latter almost twice as bad as coal.
- Even if one only burns forest residues left after logging for other purposes, emissions factors could still be similar to natural gas over a 100-year time-horizon, as these residues would otherwise naturally decay only over decades (and also add to soil carbon stores). If their fate was simply to be burned on-site, then residues are indeed a relatively low carbon energy source.
- Woody biomass taken from forests for electricity generation is, overall, probably similar or only marginally better than alternative fossil fuels in its 100-year equivalent emissions profile (and some biomass sources will be significantly worse than coal); proposed biomass projects should be evaluated on an individual basis.

Woody biomass burned for electricity is an increasing component of renewable power portfolios in the US (but still accounted for just 1.6% of total electricity generation in 2014), and especially in Europe (which is aggressively pursuing bioenergy and has begun to import wood pellets produced in the Southern US), but the ecological and climate soundness of this practice is unclear. Woody biomass is often regarded as an immediately net zero-emissions energy source, because, it is assumed, the carbon liberated from wood burning will *eventually* be re-incorporated into new biomass. This assumption is fundamentally flawed for multiple reasons, the simplest being that there is a long lag between the burning of forest matter and regrowth, implying that, at the very least, bioenergy is not immediately carbon neutral and has a short-term warming effect that is compensated for later. More fundamentally, this view fails to consider the fate of the forest in the absence of harvesting, which is generally to continue to absorb large amounts of carbon [46], with this true even for old-growth forests. Furthermore, continuous harvesting permanently reduces the amount of carbon stored in forests [150], can deplete forest soil carbon [145] and total carbon stock beyond the amount harvested [148], and may decrease forest productivity with corresponding reductions in carbon storage [143, 144].

Given all these factors, the ultimate effect of wood harvesting on the climate for bioenergy is extremely controversial, and the issue is surrounded by a great deal of genuine uncertainty. One may consult [151] or [152] for overviews of some aspects of the controversy. US forests are a major carbon sink, and offset 10–20% of the US's annual GHG emissions [46, 522]. The net effect of bioenergy harvesting on this sink is unclear. In some more arid regions, light thinning of forests could reduce wildfire risk and drought stress for net emissions reductions, but heavier harvesting is likely to undermine forest productivity and increase net carbon emissions

[143, 144]. Hudiburg et al. [143] concluded that, in the US Northwest, forest management for either fire prevention or bioenergy increased overall emissions compared to business-as-usual, with bioenergy the worst scenario.

Several recent studies that have attempted to compare the integrated warming of biomass harvested from re-growing forest have used the GWP_{bio} metric, introduced by Cherubini and colleagues [146], which purports to measure the relative warming effect of biomass versus an equivalent amount of fossil energy, and several studies have given GWP_{bio} in the 0.34–0.62 range (as reviewed in [150]), suggesting that the emissions from forest biomass are around half those of fossil fuels, although Holtsmark has derived larger values, about 1.5, for boreal forests [150]. The most obvious problem here, of course, is that fossil fuels are not a homogenous block, with combustion emissions for electricity generation from natural gas around 60% lower than from coal. Directly comparing wood-fired electricity generators, coal, and gas plants shows that the biomass emissions factor could plausibly range from as little as 0.2 kgCO₂e/kWh to almost 2.0 kgCO₂e/kWh, depending upon stand characteristics (see Section 4.10.3). Given the combustion characteristics of wood and wood-fired plants, a GWP_{bio} of 0.5 probably implies emissions similar to natural gas, while $GWP_{bio} = 1$ would be similar to coal. A recent global mapping effort by Cherubini et al. [147] yielded a global averaged 100-year GWP emission factor of 0.49 kgCO₂e per kgCO₂ released via bioenergy, again suggesting forest bioenergy may be similar to natural gas (although the global temperature potential metric was much closer to zero, reflecting the fact that most warming from wood energy occurs early in time).

My own view is that, while woody bioenergy from fast-growing stands could be better than coal or natural gas over a 100-year timeframe, this is uncertain, depending strongly upon the growth characteristics of the particular forest being harvested and the fate of the forest under alternative management, and in many cases wood is still a relatively high-carbon energy source. Intense wood harvesting would probably have broadly negative ecological effects and could markedly undermine ongoing large-scale carbon sequestration in forest ecosystems, while *light* thinning may be beneficial to *some* forests. Furthermore, unlike wind, solar, and perhaps nuclear, wood is not a scalable replacement for fossil fuels [47]. For these reasons, individual woody bioenergy projects could be beneficial but should be carefully considered with respect to local conditions, and woody biomass in general should not be viewed as a valid long-term (or even short-term) fossil fuel replacement or as a major climate change mitigant. Managing forests for carbon sequestration (which, again, may involve some degree of lighter thinning with the products used for bioenergy) rather than fuel substitution strikes me as the generally superior strategy.

Fuel mixes for wood-fired plants are variable, but generally consist of a mix of urban tree trimmings, residues from forest clearing and thinning, low-quality lumber, and pulpwood or whole live trees, harvested either from natural forest or possibly tree plantations. Note that in the past a majority of wood-fired electricity was generated in industrial wood pulp plants in combined heat and power plants that used the heat on-site, and the electricity generated was thus, at least arguably, an additional benefit that one could credit as zero-carbon, but now utilities are increasingly generating electricity from designated biomass generators and via co-firing of wood with coal.

I now review more deeply the combustion emissions from wood, and the effects of forest harvesting on forest carbon pools, atmospheric carbon dioxide, and the integrated warming effect of biomass versus fossil fuel electricity.

4.10.1 Combustion emissions

- At the point of combustion, typical wood-fired generators emit around 1.33 kgCO₂/kWh of electricity, while coal emits about 1 kgCO₂/kWh, but this fact means little in isolation of forest carbon dynamics.

As reviewed in my extensive discussion on firewood (Section 12.5.6), dry wood has a high heating value of about 5.56 kWh/kg (slightly more for softwood, slightly less for hardwood), corresponding to 11.02 kWh/kgC, assuming dry wood is 50% carbon by mass, and giving thermal combustion emissions of 0.33 kgCO₂/kWh(t). Now, wood-fired generators operate at lower temperatures than coal plants, and so thermal efficiency tends to be significantly lower (see Section 12.3 for a discussion of the Carnot Heat Engine and the importance of boiler temperature in determining engine efficiency), ranging from about 17–29%, with 24 or 25% typical [153]. This translates into combustion emissions anywhere from 1.147–1.957 kgCO₂/kWh(e), with perhaps 1.33 kgCO₂/kWh typical, and about 33% higher than coal. This by itself, of course, does not imply that biomass is a high-carbon fuel overall.

4.10.2 Overview of regrowth, carbon dynamics, and carbon payoff following harvesting

Harvesting forest biomass affects multiple carbon pools, and such changes must be considered in reference to a baseline counterfactual scenario where no harvest occurred. One method of carbon accounting, a “carbon-balance” approach, invokes the concepts of (1) carbon debt repayment, and (2) carbon sequestration parity, as shown schematically in Figure 4.15 [151]. We see that, because forests are likely to continue growing and absorbing carbon in the absence of harvesting, even once one has re-paid the carbon debt of harvesting compared to the pre-harvest forest mass, there is still a large debt relative to the counterfactual of no harvesting. True “carbon neutrality” is not reached until the carbon sequestration parity point (see Figure 4.15). However, as we shall see, even at this point, the cumulative warming effect of the harvesting scenario can be greater than the no-harvest scenario, and a “warming-debt” may still exist long after carbon parity.

While the carbon-balance approach is valid, it does little to tell us the absolute warming effect, either before or after reaching the carbon sequestration parity point, of biomass: what we would really like is to have a GWP-like metric for a more direct comparison to fossil fuels. Towards that end, several authors (e.g. [146, 150]) have used an alternative metric, the GWP_{bio}, as a means to quantify the warming effect of forest biomass compared to an equivalent amount of fossil energy. In the following section, I derive an expression for GWP_{bio} from a relatively simple mathematical model of forest growth and harvesting, and I offer my critique and modification of this metric.

4.10.3 A simple mathematical model for harvesting and biomass GWP

To gain some more direct insight, I follow several works by Holtsmark [149, 150] to explicitly describe the dynamics of live forest biomass, harvest residues, deadwood, and soil carbon, with and without harvesting. This model considers four carbon pools: (1) total live biomass, $B(t)$, (2) tree stem biomass, $G(t)$, which is some fraction, θ , of total biomass, assumed to be 48%, (3) natural deadwood, $D_N(t)$, and (4) deadwood as a harvest residue, $D_R(t)$. I take all variables to have units MgC (i.e. the absolute amount of carbon in each pool). We can model the growth

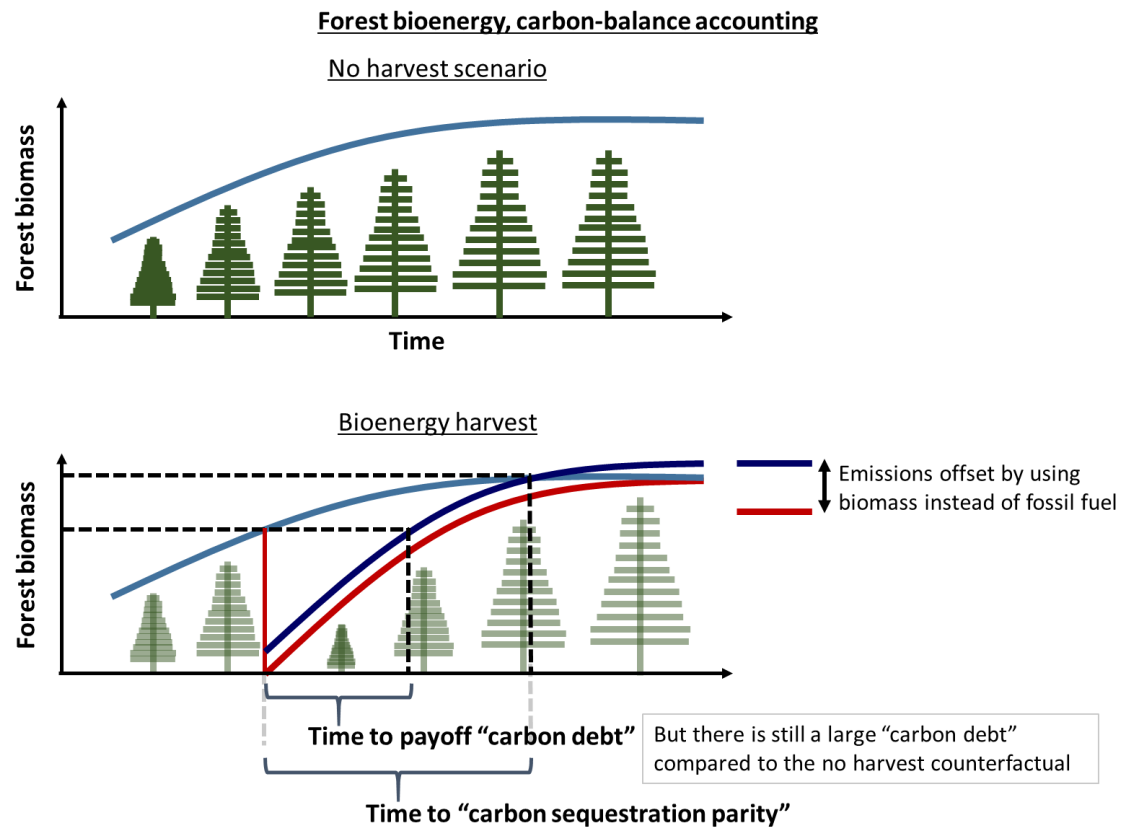


Figure 4.14: Schematic for the carbon-balance accounting method of assessing the carbon impact of woody bioenergy derived from forests. See also Figure 2 of [151]. At the point of harvest, forest biomass goes to zero (at least in schema, as shown by the red line), while some amount of fossil carbon is offset via the use of forest products for energy generation, and so net carbon storage is given by the dark blue line. With forest regrowth, equivalent carbon stores eventually match the pre-harvest forest (payoff time for the carbon debt), but it is not until equivalent stores equal to forest carbon stored under the counterfactual of continued growth that carbon sequestration parity is reached.

of tree stems with a Logistic function

$$G(t) = \nu_1 (1 - e^{-\nu_2 t})^{\nu_3}, \quad (4.1)$$

where ν_1 , ν_2 , and ν_3 are parameters particular to any tree stand. Since θ is the fraction of live biomass that is stem, $B(t)$ follows simply as

$$B(t) = \frac{1}{\theta} G(t). \quad (4.2)$$

Natural deadwood is generated by live biomass, and we have litterfall given as βB , while we suppose first-order decay of deadwood at rate ω , yielding

$$\frac{dD_N}{dt} = \beta B - \omega D_N. \quad (4.3)$$

Now, if we harvest tree stems at time t_h , and σ is the fraction of non-stem residue (e.g. tree tops, stumps) taken with the harvest, then we extract (in MgC)

$$E(t_h, \sigma) = G(t_h) + \sigma(B(t_h) - G(t_h)). \quad (4.4)$$

That fraction of residue not taken, $1 - \sigma$, remains in the forest as residue deadwood, $D_R(t)$ and decays at first-order rate ω , giving

$$D_r(t, t_h, \sigma) = e^{-\omega t} (1 - \sigma) (B(t_h) - G(t_h)). \quad (4.5)$$

Now, we can calculate the net atmospheric carbon over time that results either without a harvest (given current forest conditions), or with a harvest of prescribed magnitude (e.g. clear-cut, light harvest, etc.) with stand regrowth according to the equations above, using the standard equations describing CO_2 concentration following a CO_2 bolus, and with $y(t)$ representing the concentration time-course for a single kg CO_2 bolus (see Section 3.3.1, or complete details in [149, 150]). If $C_0(t)$ is the atmospheric carbon (not CO_2) time-course without harvesting, and $C_H(t)$ is the time-course with harvest, then from the concentration difference,

$$C(t) = C_H(t) - C_0(t), \quad (4.6)$$

we can determine the additional integrated radiative forcing, $\text{AGWP}_{\text{bio}}(t)$, as

$$\text{AGWP}_{\text{bio}}(t) = \int_0^t A_{\text{CO}_2} \frac{44}{12} C(s) ds, \quad (4.7)$$

where A_{CO_2} is the radiative efficiency of CO_2 . Now, the GWP_{bio} metric, as used by Holtmark [150], Cherubini [146], and others has been taken as

$$\text{GWP}_{\text{bio}}(t) = \frac{\text{AGWP}_{\text{bio}}(t)}{\text{AGWP}_{\text{CO}_2}(t)}, \quad (4.8)$$

where $\text{AGWP}_{\text{CO}_2}(t)$ is the integrated radiative forcing that results directly from the combustion of the forest harvest

$$\text{AGWP}_{\text{CO}_2}(t) = \int_0^t A_{\text{CO}_2} \frac{44}{12} E(0, \sigma) ds, \quad (4.9)$$

assuming harvesting at time 0. Typically, $\text{AGWP}_{\text{CO}_2}(t)$ has been interpreted as the warming that would have, without combustion of wood, resulted from an equivalent degree of fossil fuel combustion, and therefore $\text{GWP}_{\text{bio}}(t)$ gives us the relative amount of warming, at any particular time, resulting from using forest wood over fossil fuel [146, 150]. If $\text{GWP}_{\text{bio}} < 1$, then wood is

less warming, while if $\text{GWP}_{\text{bio}} > 1$ then fossil energy is better, and, in keeping with the IPCC GWP framework, it is probably most appropriate to evaluate GWP_{bio} at 100 years post-harvest.

However, this interpretation of GWP_{bio} is fundamentally flawed, in my view, as it implicitly assumes that a carbon atom from biomass corresponds to exactly the same amount of electricity (or heat, or automotive power, etc.) as a carbon atom from fossil fuel. This is obviously false, as the intrinsic heat content of wood is lower than that of fossil fuels (i.e. 1 kg of wood carbon yields less energy than 1 kg of fossil carbon), the efficiency of wood-fired power plants is significantly lower than that of typical fossil plants, and fossil fuels themselves vary markedly in their emissions profiles (e.g. coal vs. natural gas). Fortunately, it is a fairly simple matter to account for these factors, and we can simply derive $\text{kgCO}_2\text{e/kWh}$ emissions factors for bioenergy that are directly comparable to similar EFs for any fossil fuel, as follows.

Given E , the mass of carbon harvested, we determine the amount of electricity generated, assuming a HHV of 11.02 kWh/kgC and a power plant thermal efficiency of 25%. Given the kWh produced, which we denote E_{kWh} , we then use the formula

$$\text{EF}(t) = \left(\frac{1}{E_{\text{kWh}}} \right) \left(\frac{\text{GWP}_{\text{bio}}(t)}{\text{AGWP}_{1\text{kgCO}_2}(t)} \right), \quad (4.10)$$

to yield a time-dependent emissions factor with units $\text{kgCO}_2\text{e/kWh}$, with $\text{AGWP}_{1\text{kgCO}_2}(t)$ the integrated RF from a single kg of CO_2 . Since we have already constructed time-dependent emissions factors for coal and natural gas (see Figure 4.8 in Section 4.6.1), we can directly compare electricity generation from forest products to these two fossil fuels, which I do in a moment, finding that forest bioenergy is generally just as bad as fossil energy. Note that in the following results, I have omitted any negative perturbation of the forest soil carbon pool by harvesting (this was considered by Holtsmark [150]), and so they are actually biased in favor of bioenergy.

Model results and emissions factors

Figure 4.15 shows the evolution of different forest carbon pools following clear-cutting of the trees, with 75% of harvest residues left to decompose in the forest, along with the total change in atmospheric CO_2 resulting from this clear-cut, compared to the counterfactual of leaving the forest be. I use parameter values from [150], including ω (decay rate for deadwood) at 0.04 year^{-1} .

Figure 4.16 compares forest growth dynamics, and equivalent emissions factors, when harvesting either a slow-growing boreal forest with either clear-cutting, heavy harvesting, or light harvesting, or a faster-growing forest under the same set of harvests. Note that the emissions factor actually increases early in time: this is due to carbon released via decay of residual deadwood. We see that harvesting from slow-growing forests is often worse than coal, while fast growing forest biomass is comparable to or better than natural gas by the 100-year mark.

Finally, let us model a common scenario, and one that has often been viewed as a net zero-emissions activity, namely the use of unmarketable residues (branches, tree-tops, etc.) from a lumber harvest for energy. As pointed out by Ter-Mikaelian et al. [151], such residues are often left to decay naturally, and even when burning is a common practice, often less than 50% of slash piles are actually set afire. In any case, I find that, compared to the counterfactual of simply leaving residues to rot, the residue 100-year EF is on the order of $0.3 \text{ kgCO}_2\text{e/kWh}$ for a first-order decay rate of 0.04 day^{-1} , as used by Holtsmark [150], and closer to $0.6 \text{ kgCO}_2\text{e}$ when $\omega = 0.02 \text{ day}^{-1}$, which is a more likely overall average for coarse woody debris [559]. If the counterfactual scenario is burning about half of residues on-site, then these EFs are in the $0.1\text{--}0.3 \text{ kgCO}_2\text{e/kWh}$ range, which is indeed fairly low carbon. However, not modeled here is

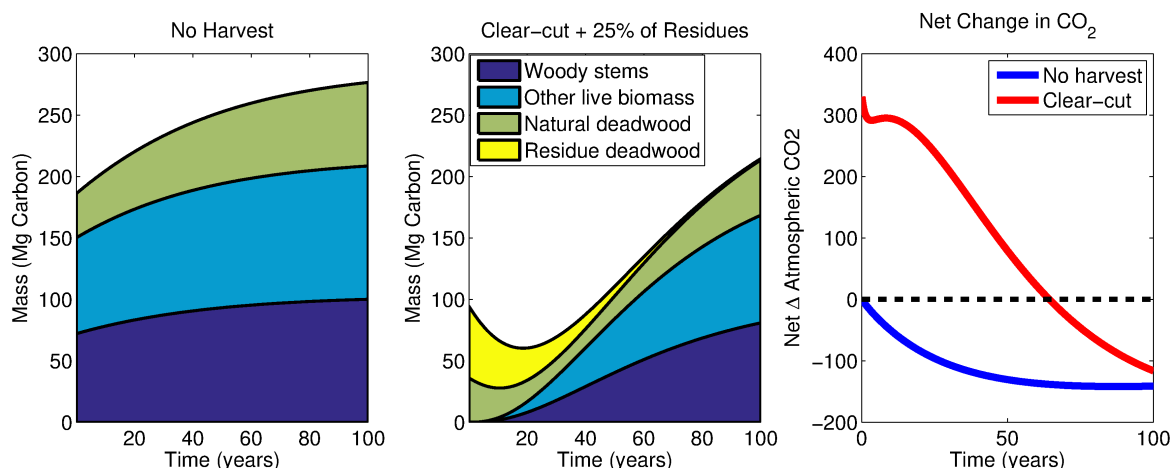


Figure 4.15: Approximate carbon pools for a slow-growing boreal forest either under no harvesting (left panel) or under clear-cutting of the woody stems, leaving 75% of harvest residue (branches, stumps, etc.) to decay in place (middle panel). The right panel shows the net change in atmospheric CO₂ under either scenario: without harvesting the forest continues to slowly take up carbon, while harvesting results in large early CO₂ release that is eventually mostly compensated for.

the effect residue harvesting has on depleting forest soil carbon pools, which Repo et al. [145] found to be quite significant.

Now, the above results do not account for forest soil carbon dynamics, the inclusion of which makes bioenergy even more unfavorable [150, 145]. Additionally, the logistic growth model assumes that old-growth forests stop taking up carbon, an assumption that is probably false. Harvesting also can decrease forest productivity, and continuous harvesting leads to a permanent forest carbon deficit. Accounting for any of these behaviors would lead to higher emissions factors for biomass. Furthermore, I have not considered any of the energy/emissions required for harvesting, power plant construction, or the forest land that must be cleared for access roads, etc. Therefore, I feel fairly confident in the conclusion that biomass electricity is closer to fossil fuels in its emissions profile than it is to other major renewable energy sources.

4.10.4 eGRID correction

I use 500 gCO₂e/kWh as an extremely crude eGRID correction, given the great uncertainty as to the true impact of biomass on climate.

4.11 Geothermal

Geothermal power plants generated only 0.37% of all US electricity in 2010 (eGRID), but geothermal plants are a significant source of energy in California and Nevada, where they generated 6.17% and 5.89% of all electricity, respectively. Non-trivial geothermal capacity exists only in three other US states, namely Hawaii, Utah, and Idaho, where it accounted for 1.85%, 0.66%, and 0.60% of electrical generation, respectively. Geothermal plants convert the heat of geofluids from great depths to electricity, and conventional plants are all installed over geologically young and active areas containing unusual reservoirs of hot geofluids located relatively close to the surface. In general, wells are drilled to a depth of 1–3 km, and superheated fluid or steam is pumped to the surface, where it drives turbines that in turn generate electricity.

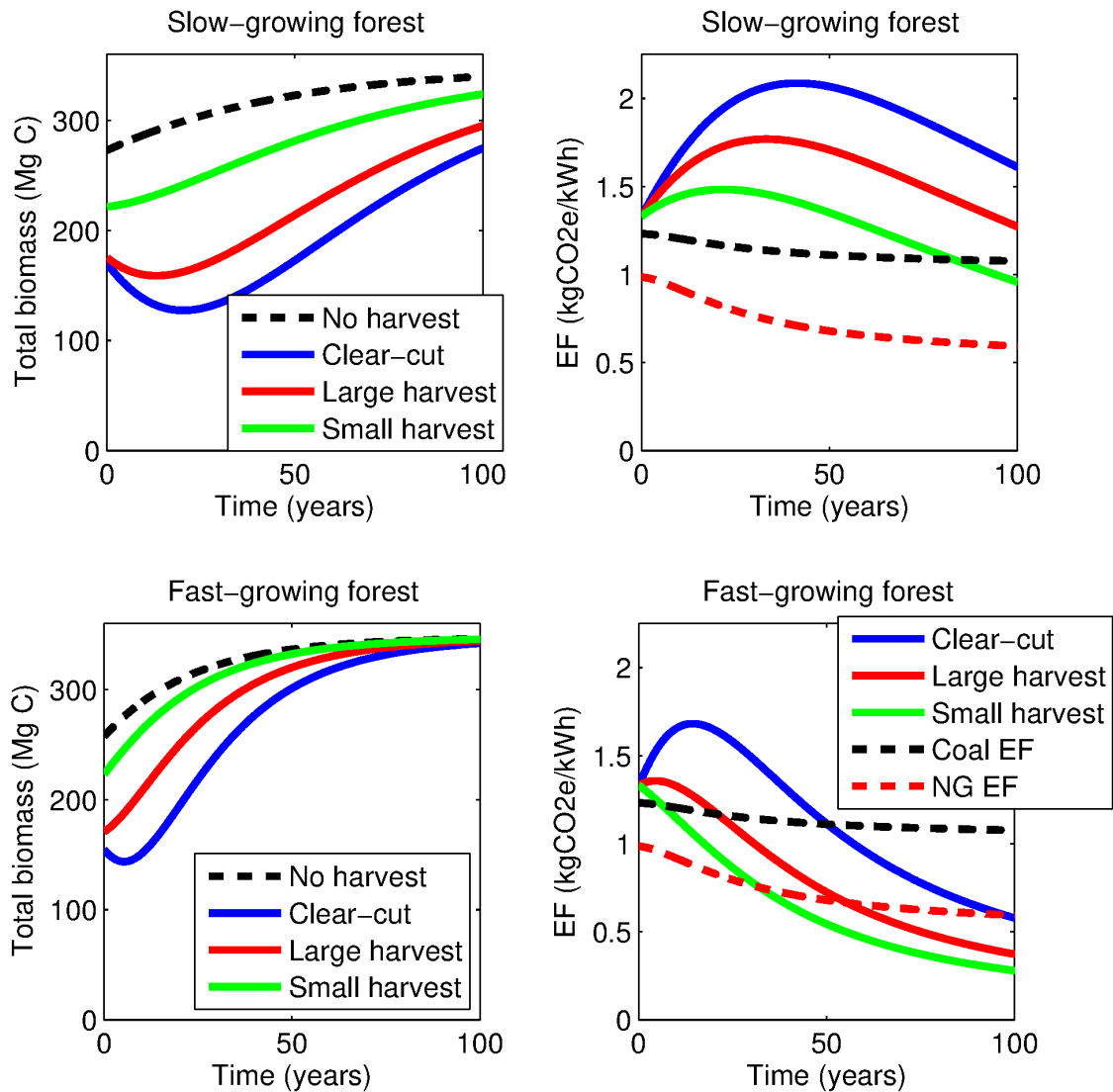


Figure 4.16: Changes in forest biomass and equivalent kgCO₂e/kWh emissions factors, when forest biomass is harvested for electricity generation. The top gives results for a slow-growing forest, showing that this scenario may be worse than coal even out to 100 years, while the bottom panels show results for a fast-growing forest, where lighter harvests are clearly superior to natural gas at the 100-year horizon. Even in the fast-growing forest case, it is still generally at least 50 years before any benefit to bioenergy over fossil fuels becomes manifest.

Cooled fluid is then pumped back via an injection well to replenish the geothermal reservoir.

There are three major classes of conventional geothermal plants—dry steam, flash, and binary—each designed for use with steam/fluid of different temperatures. Dry steam plants are employed in the hottest areas, where superheated steam is directly pumped from the well to drive a turbine. Flash plants use superheated fluid that is composed of a mixture of liquid and vapor; the mixture is “flashed” via centrifugal action separating the two phases, and the resulting vapor drives a turbine. The liquid may be flashed a second time (“double-flash” plant) to increase efficiency. Binary plants use the coolest geofluids ($< 150\text{ }^{\circ}\text{C}$), which are pumped through a heat exchanger to transfer heat to a secondary fluid with a lower boiling point; this secondary fluid vaporizes and drives a steam turbine.

All dry steam plants in the US are located in the Geysers, the largest geothermal field in the world, located just north of San Francisco. This field alone accounts for about 55% of CA geothermal capacity and 47% of overall US capacity. Most flash plants in the US are also located in CA, while outside CA, most plants are of the binary type, and nearly all growth in geothermal power over the last 20 years has been in binary generation. California accounts for 83% of US geothermal power, and 93% of steam and flash power [156].

Geofluids contain significant quantities of non-condensable greenhouse gases. In binary plants, the secondary fluid cycles in a closed loop through the vapor and liquid phase, while the geofluid is extracted and re-injected without ever making contact with the atmosphere. Thus, binary fluids are considered to have operating emissions that are effectively zero [156]. In contrast, the geofluid in steam and flash plants comes into direct contact with the atmosphere, allowing significant fugitive CO_2 and CH_4 emissions to occur.

A 2003 survey of US geothermal plants by Bloomfield et al. [157] reported a weighted average of $90.7\text{ gCO}_2/\text{kWh}$ and $0.753\text{ gCH}_4/\text{kWh}$ ($25.6\text{ gCO}_2\text{e}/\text{kWh}$, using GWP 34), for an overall average of $116.3\text{ gCO}_2\text{e}/\text{kWh}$. Assuming that the emissions from binary plants (14% of generation in 2003) are nil, we have an EF of $135.3\text{ gCO}_2\text{e}/\text{kWh}$ (including $29.8\text{ gCO}_2\text{e}/\text{kWh}$ due to methane) for steam and flash plants. A widely cited work by Bertani and Thain [155] reportedly sampled 85% of 2001 world generating capacity, and reported a range of $4\text{--}740\text{ gCO}_2/\text{kWh}$ with a weighted average of $122\text{ gCO}_2/\text{kWh}$ (see discussion in either [156] or [154], I have been unable to locate the original work); this survey considered CO_2 only, omitting any methane emissions. Other estimates are thoroughly reviewed in a recent overview by Bayer et al. [154].

Recently, Sullivan and colleagues extended the GREET model to incorporate geothermal energy [156]. They concluded that plant-cycle (i.e. emissions from plant construction, well-drilling, etc.) are insignificant, at perhaps $4\text{ gCO}_2\text{e}/\text{kWh}$ for steam/flash plants, and $6\text{ gCO}_2\text{e}/\text{kWh}$ for binary plants. Using data reported to CARB, they further concluded mean emissions of $97.9\text{ gCO}_2\text{e}/\text{kWh}$ for operating plants in California; it is unclear if this data includes methane emissions or represents CO_2 emissions alone. Given this uncertainty, and the fact that this estimate is lower than other major estimates cited above, I suggest an EF of $125\text{ gCO}_2\text{e}/\text{kWh}$ for steam/flash plants, and an EF of $6\text{ gCO}_2\text{e}/\text{kWh}$ for binary plants. Binary generation by state is 6%, 25%, 63%, 100%, and 100% for CA, UT, NV, HI, and ID, respectively [156]. Since eGRID subregions do not partition strictly by state, however, and since most geothermal energy is generated in California where binary plants are rare, I use an eGRID correction of $115\text{ gCO}_2/\text{kWh}$ across the board.

4.12 Wind

- Wind power has the lowest embodied carbon emissions of any major power source: the likely range for utility-scale wind is 10–30 gCO₂e/kWh.
- Other negative environmental impacts, mainly bird and bat deaths, are of concern but are probably low compared to fossil-fuel power plants (and other human activities and structures), although harms to bat populations in particular remain poorly understood.

Wind power probably has the lowest lifecycle emissions of any electricity source, likely in the 10–30 gCO₂e/kWh range for utility-scale wind. This source has rapidly scaled up in recent years, increasing from less than 0.5% of US generation in 2005 to 4.3% in 2014 (World Bank), and wind is becoming a major power source in the Midwest: South Dakota and Iowa both derived about 25% of their electricity from wind in 2012, while in six other states wind was at least 10% of the generation mix (eGRID).

Wind has been generally viewed, accurately, as a truly low carbon energy source with relatively low environmental harms. It remains true that wind farms can negatively affect wildlife, and increased bird and bat mortality due to collisions with turbines has been fairly widely publicized. As discussed below, wind turbines may actually be safer overall for birds (per kWh generated) than fossil fuel plants, but this hazard may be greater for bats and should be considered when siting future wind farms. By harvesting significant amounts of wind energy and inducing turbulence, very large-scale wind farming also has the potential to alter regional climate and ground surface temperatures, but these effects are very minor [158].

I briefly introduce the physics of wind turbine, review lifecycle greenhouse emissions, turn to a brief discussion of the scalability of this intermittent power source, and close with a discussion of other negative environmental impacts.

4.12.1 Wind harvesting fundamentals

Wind resources

On a planetary scale, wind is generated by sunlight, which disproportionately heats air near the equator, inducing it to rise and move toward the poles, and by the Coriolis force from Earth's rotation. The latter induces clockwise rotation in the Northern Hemisphere, and counter-clockwise rotation in the Southern Hemisphere. At the local scale, the landscape strongly affects winds, with rougher surfaces (e.g. cities) significantly slowing air flow; because wind speed must equal zero at ground level, we also have a boundary layer effect such that wind speed increases with vertical height for several hundred meters. At low altitude, wind speed, V , increases logarithmically with height,

$$V \propto \log \left(\frac{z}{z_0} \right) \quad (4.11)$$

where z is height, and z_0 is the *roughness* (measured in m) of the terrain, and may be 10–100 over mountains, 0.5–2 over cities and forests, 0.01 over plains, and 0.0001–0.001 m over the sea. This helps explain why wind resources in the US are greatest off-shore and over the Great Plains region, as depicted in Figure 4.17, and why turbines towers are typically 35–125 meters in height (not including the rotors), with newer installations and off-shore turbines trending higher and higher.

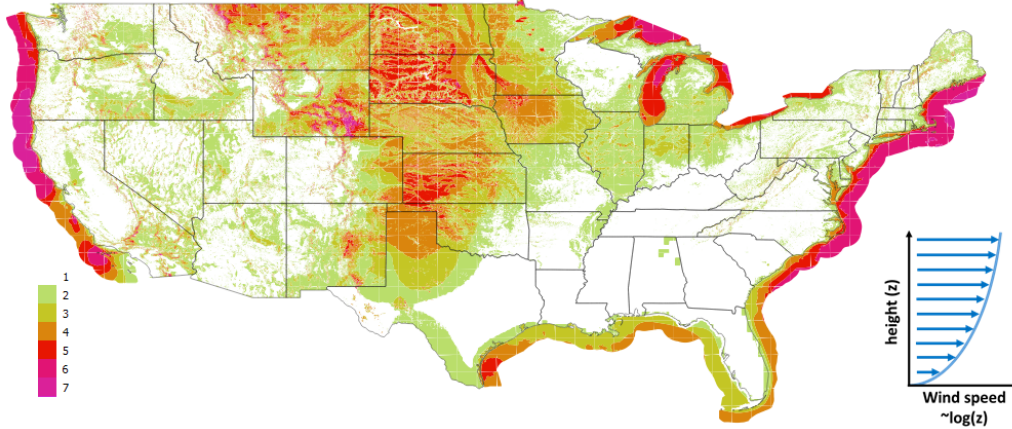


Figure 4.17: Map of wind resources in the US, which are concentrated in offshore and the Great Plains regions. Also inset is the logarithmic relationship between height and wind speed. Map data is from publicly available NREL databases.

Maximum harvestable wind: from individual turbines to the regional scale

The amount of power that a turbine generates is proportional to the rotor area, air density, and wind speed cubed, and it can be shown that it is theoretically impossible for a turbine to extract more than 59% of the power in wind (the *Betz Limit*) [162]. To see this, first note that the kinetic energy contained in a mass of air of volume V moving at velocity u is given as

$$E = \frac{1}{2} \rho V u^2, \quad (4.12)$$

where ρ is the density of air. If this air is moving through a circular cross-section such as, say, a turbine rotor, of area A , then it moves at volumetric rate $dV/dt = Au$, and the power of the moving air is

$$P = \frac{dE}{dt} = \frac{1}{2} \rho A u^3. \quad (4.13)$$

Now, when a parcel of air passes through a rotor that harvests energy, we must have that both the velocity of exiting air decreases, while the cross-sectional area increases (a consequence of the conservation of mass). Since the air cannot exit at velocity 0 (the passage of air would cease), nor can it maintain the same velocity (no energy should be harvested in this case), power will be optimally extracted when the exit velocity, u_2 , is some non-zero fraction of the wind stream velocity, u_1 . By arguments outlined in Figure 4.18, this optimum occurs when $u_2 = u_1/3$, at which point the power coefficient, C_p , i.e. the fraction of power extracted, is exactly $19/27$, or about 0.59. This maximum is known as the “Betz Limit.” There are additional limits on power extraction related to rotational inertia, and one may consult Grogg [162] for a far more detailed treatment.

Since wind is markedly slowed and as much as 50% of its energy extracted upon its encounter with a turbine, to place turbines in close succession would be fey, and so these giants must array themselves across many leagues. Significant extraction of kinetic energy from wind, combined with limited replenishment from higher altitude winds, acts to limit large-scale wind electricity generation to about 1 W m^{-2} in windy regions of the US [159]. For perspective, this harvesting rate over the entire area of Kansas (213.1 billion m^2 , or 2.8% of the Continental US) would yield 1.87 billion MWh/year, or a little under half annual US electricity generation; it would similarly

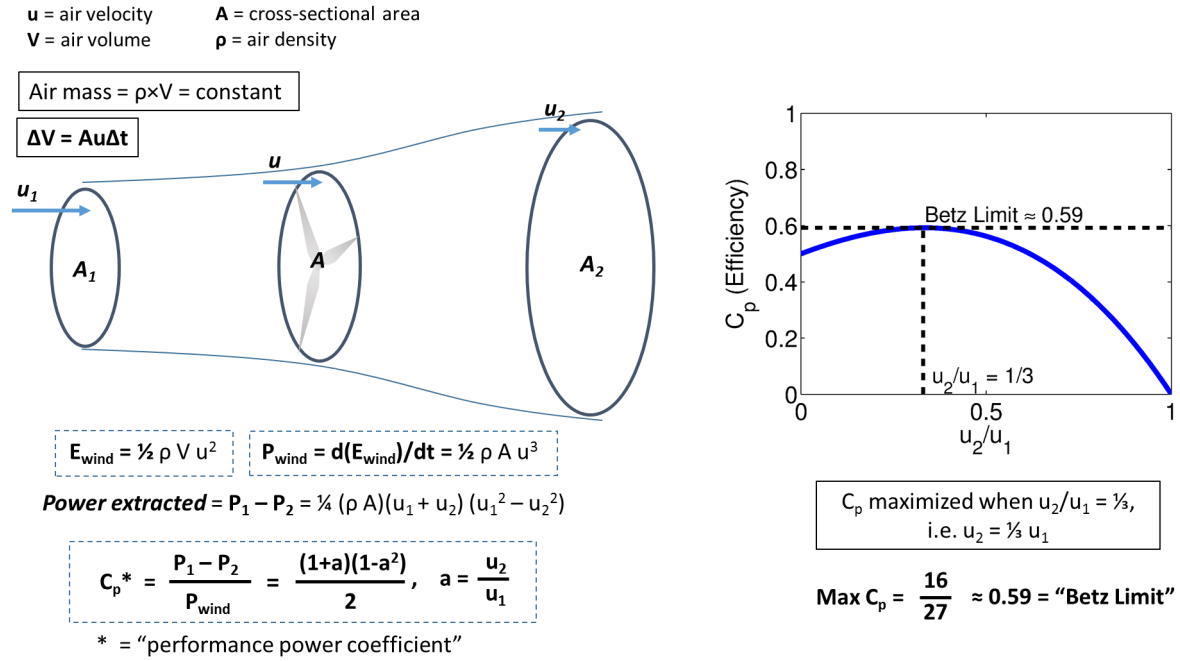


Figure 4.18: Outline of the physical argument underlying the Betz Limit, the maximum fraction of power that may be harvested from a wind stream by a rotor. This maximum is extracted when the exit air stream's velocity is one-third that of the entering stream, and is equal to exactly 19/27, or about 0.59.

take about one-third of Texas to provide half the US's electricity⁵. Since turbines themselves take up only a very small fraction of the land area harvested for wind, and may be placed on land co-used for agriculture, this land footprint is not in itself prohibitive.

Capacity factor

The *nameplate capacity* gives the maximum power output of a turbine, while the *capacity factor* is the ratio of actual power generated to nameplate capacity. For example a 2 MW turbine with a capacity factor of 0.30 will, on average, generate 0.6 MW, yielding 5,256 MWh of electricity annually. The average capacity factor for US wind power was 0.325 in 2015, per the EIA. The capacity factor obviously varies with location, but it is generally larger for larger turbines, as they reach the higher and faster winds [160].

⁵Per the American Wind Energy Association, installed wind capacity in 2014 was 61,327 MW. Assuming a capacity factor of 34% (EIA) and a maximum of 1 W per m^{-2} , this implies about 20.9 billion m^2 of land were devoted to wind-farming in 2014, or just under 10% of the area of Kansas (of course, <1% of this land is actually turbine).

4.12.2 Lifecycle GHG emissions

- Utility-scale turbines generate on the order of 20 gCO₂e/kWh or less over a 20-year lifecycle, and the initial carbon investment is usually paid off within six months.
- Small residential-scale wind installations are slightly more carbon-intensive, but still low-carbon overall (perhaps 50 gCO₂e/kWh for a grid-tie system, and >100 gCO₂e/kWh for an off-grid system with batteries).

The harvesting of wind energy generates no emissions directly, but turbines are massive structures whose fabrication requires up to several thousand tonnes of carbon-intensive materials. Nevertheless, the literature is uniform in finding that the overall impact is ultimately nearly trivial for most turbines: a review by Arvesen et al. [160] gave 19 ± 13 gCO₂e/kWh, Dolan et al. [163] gave a range of 3.0 to 45 gCO₂e/kWh with a median of 11 gCO₂e across 126 estimates (after harmonization), and Nugent and Sovacool give an average of 34.1 gCO₂e/kWh across 41 studies [165].

Carbon emissions come from (1) material production, (2) materials transport and turbine construction/assembly, (3) operation and maintenance, and (4) decommissioning after a roughly 20-year service life. Materials, especially steel and concrete, are the major source of embodied carbon emissions. Decommissioning, while requiring some energy, acts overall to offset some lifecycle emissions if steel, iron, and other metals are recycled. The relative GHG impact of these categories is summarized in Figure 4.19, and Figure 4.20 shows the material makeup of one large 2 MW geared turbine, based on [166].

A general trend seen in LCAs is one toward lower lifecycle emissions for larger turbines. As noted above, larger/taller turbines tend to have higher capacity factors [160], and it is generally more efficient on a materials basis to build a single turbine with a high capacity than multiple smaller turbines [161]. However, this trend is slight and disappears once turbines reach the MW scale (see Figure 4.19), and even very small-scale residential installations are likely to emit only around 50 gCO₂e/kWh, comparable to rooftop solar. Note that *off-grid* residential wind-systems will have significantly higher lifecycle emissions, due to the need for batteries. For example, one study [164] of an off-grid installation suggested 116.3 gCO₂e/kWh, 61% of which was attributable to the battery system (although even this is still very low compared to fossil energy).

Finally, the carbon payoff time for large-scale wind turbines is less than one year, and likely only a few months. Suppose a 2 MW turbine has associated lifecycle emissions of 2,000 MgCO₂e and operates with a capacity factor of 0.30, generating 5.256 million kWh/year. Assuming it displaces grid-average electricity, then the entire initial carbon investment is paid off in 6.6 months (displacing marginal electricity, and we have payoff at 4.9 months). Note that this example turbine has 19 gCO₂e/kWh amortized over a 20 year lifetime.

For corrected eGRID emissions, I use an EF of 19.0 gCO₂e/kWh for wind power.

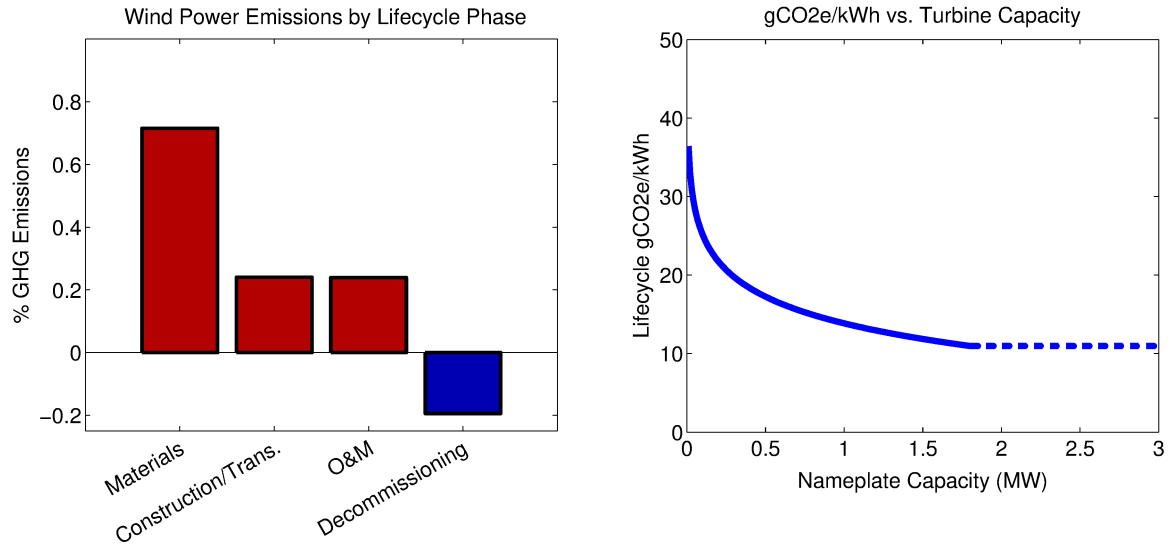


Figure 4.19: The left panel shows the relative contribution to GHG emissions from each major phase of the wind turbine lifecycle (based on [165]). The right panel shows that turbines with lower nameplate capacities tend to have higher associated emissions (based on the relation given in [160]).

4.12.3 Other externalities

Bird and bat mortality

- Wind power does kill birds via collisions, but probably causes fewer overall deaths than fossil power (coal, in particular), for a net benefit to birds. Bat mortality due to turbines is more concerning and less well-understood.
- Wind turbines are responsible for only about 0.015–0.035% of about one billion annual bird deaths attributable to (American) Man.

Bird deaths from wind turbines are probably the best-publicized downside to this power source, and there are likely several hundred thousand such deaths yearly [171]. However, analyses by Sovacool [168, 169] suggested that, both in absolute terms and per kWh of electricity, fossil fuel plants kill far more birds (including direct collisions with cooling towers, power lines, etc., and other ecological effects from fossil fuel extraction and combustion, e.g. mountain-top removal for coal mining), implying wind power is actually an overall boon to birds in terms of direct mortality (although one may wish to read Waldien and Reichard [170] for a clear-minded critique of this work). Furthermore, climate change, driven largely by fossil power plants and countered by wind power, represents a long-term, fundamental threat to the survival of myriad bird species [169].

All this being said, turbine-related avian mortality varies widely with season, location, and species, and wind farms can be very destructive to local bird populations. In particular, California demonstrates much higher mortality than the Great Plains region, and raptors, which rely on thermals, are especially vulnerable to turbines [171]. Therefore, appropriate siting is an important consideration for future installations [167]. Regional avian mortality rates for wind power, along with comparison values for nuclear and fossil power plants are given in Figure 4.21.

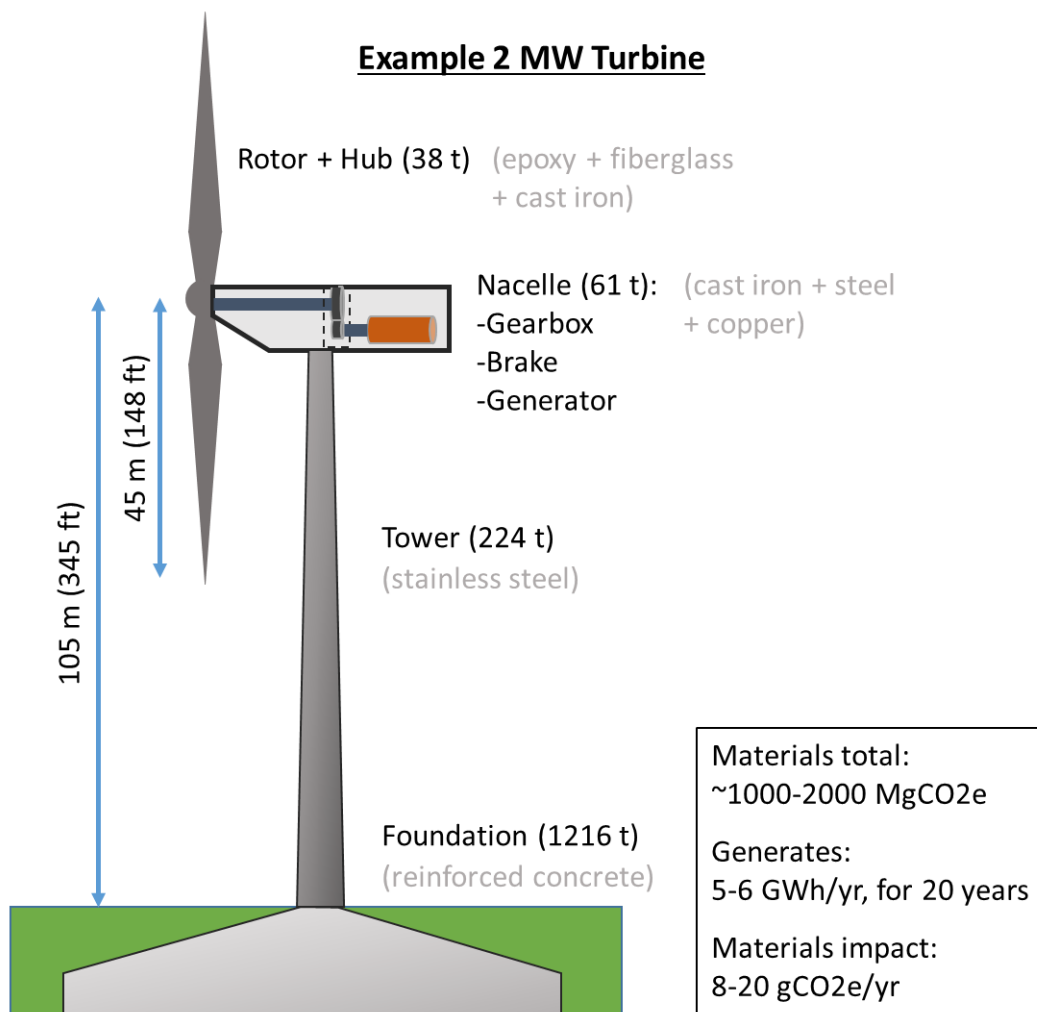


Figure 4.20: Basic schematic, materials requirements, and approximate materials carbon footprint for an example large 2 MW turbine, based on data presented in [166].

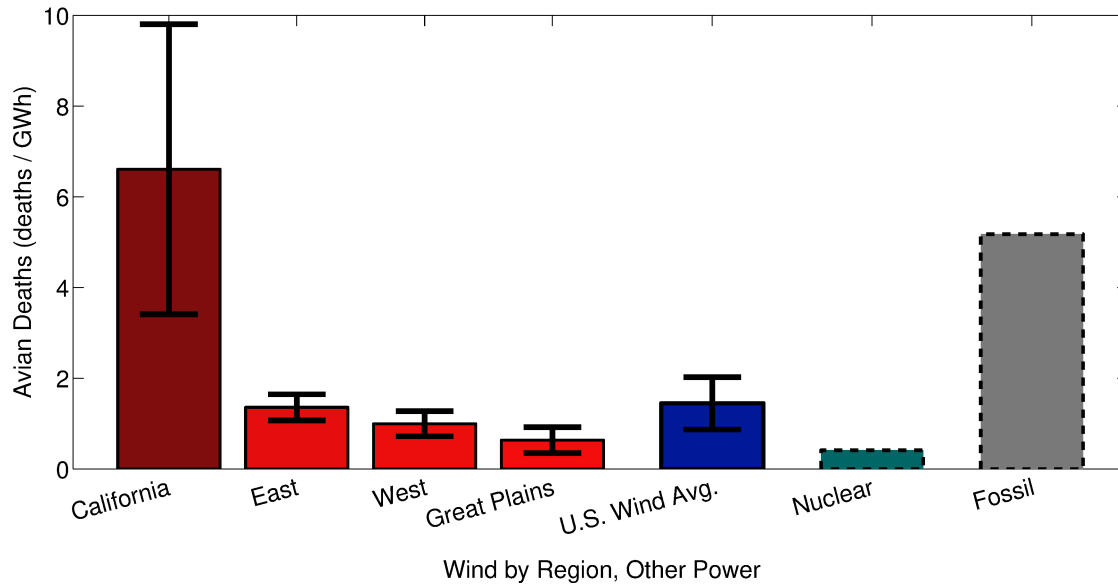


Figure 4.21: Approximate avian deaths per annual GWh of electricity generated by wind for four different regions and as an overall US average, based on [171] (deaths per MW capacity given by [171] have been converted to annual GWh assuming a capacity factor of 32.4%). For comparison, avian deaths from nuclear and fossil power derived by Sovacool [169] are included, but are very uncertain. Note that, fortuitously, the Great Plains have both the lowest avian death rate and the greatest wind power potential.

Bat mortality from turbine collisions is less understood, but is potentially much more concerning, since even though overall death rates may be comparable to those from birds [172], only three major bat species are affected (compared to thousands, for birds), bats do not interact with turbines in the same manner as birds (e.g. bats may be attracted to turbines as potential roosts), and installations in some landscapes could result in very high mortality [172].

Finally, power plants of any kind are a relatively minor hazard to birds, with buildings and windows killing about *twenty times* as many birds as all power plants (including wind) put together [167]. Electrical transmission lines, however, are major bird killers. Of the nearly *one billion* bird deaths attributable to human activity each year (just in the US), wind power causes perhaps 0.015–0.035% (based on [171] and [167]).

Direct climate effects

The turbulent wake of turbines mixes near-surface air to cause daytime cooling and nighttime warming, and wind harvesting may affect local to regional weather and precipitation patterns [174]. The net effect of harvesting wind for 100% of civilization’s energy needs could be to very slightly increase global mean temperature (about 0.1 °C) and slightly reduce precipitation (1%) [173]. Recent climate models have confirmed that temperature and precipitation effects are extremely minor on both a regional [174] and global scale [158], under any remotely plausible wind power deployment scenario.

4.13 Solar

While solar panels generate no greenhouse gases during their operation, they are not completely carbon free, as manufacture, materials mining, and maintenance have associated carbon

emissions. Most emissions occur from electricity use at the manufacturing stage, where the magnitude of emissions is also dependent on the energy mix of grid electricity. At both the global and US scales, most panels are constructed from crystalline silicon (c-Si), and this is the only solar technology scalable to a significant fraction of global energy use. On average, within the US, c-Si panels likely have associated carbon emissions of about 40–50 gCO₂e/kWh amortized over a 30-year system lifetime, or <5% of the carbon impact of coal. Furthermore, this figure is likely falling with improving technology, and will be lower in sunnier areas of the country, especially the Southwest, where the same panels may generate around 33% more energy over their lifetime as compared to the US average. In this section, I first introduce the physical fundamentals of the solar cell and fundamental limits to its efficiency, and then review the lifecycle carbon emissions associated with solar power.

4.13.1 Basics of solar PV

Several parameters describe the characteristics of a solar system. The *solar irradiance* (or insolation), is the amount of energy that falls upon a unit of area in a given amount of time, and is typically expressed in units of kWh/m²/year. Irradiance varies from as little as 1,000 kWh/m²/year in northern European countries to 2,400 kWh/m²/year in the American southwest; 1,800 kWh/m²/year is the US average, and 1,700 kWh/m²/year is the average for southern Europe [177, 179]. The *conversion efficiency* gives the fraction of incident energy that is converted into electricity, and is in the range of 14–21% for commercial PV panels. For example, one square meter of panels with a conversion efficiency of 15%, and located in the southwest (solar irradiance of 2,400 kWh/m²/year), would yield 360 kWh in a single year. Conversion efficiency varies with panel type, and is likely to continue to increase in the coming years.

Operational factors such as varying weather conditions and shade can decrease actual solar PV output, and the ratio between actual and maximum power output is referred to as the *performance ratio*. Standard values are 0.75 and 0.8 for rooftop-mounted and ground-mounted systems, respectively [177]. Thus, applying a performance ratio of 0.75 to the previous example, the actual energy generated by one square meter of panels would be 270 kWh instead of the theoretical max of 360 kWh.

4.13.2 Physical fundamentals

Modern solar photovoltaics are based on p-n semiconductor junctions, which spontaneously convert sunlight to electrical current, with silicon the fundamental semiconductor material for almost all PV technology. The essential idea of a silicon solar cell is that (1) light striking silicon generates free electrons (a consequence of the “photoelectric effect,” the discovery of which earned Albert Einstein the 1921 Nobel Prize in physics), (2) there is a permanent difference in electrical voltage across the p-n semiconductor junction, and therefore (3) free electrons flow across this voltage difference, generating an electrical current which can be attached to an external load.

To understand this process more fully, first recall from basic chemistry that electrons surrounding an atomic nucleus are restricted to certain “orbitals” which can contain only a fixed number of electrons, proceeding outward from the nucleus in “shells.” Silicon (Si), like carbon, has four “valence,” i.e. outermost, electrons, but to completely fill its outermost orbitals requires eight electrons. Thus, these four electrons can interact to form bonds and a tetrahedral crystal lattice, as illustrated in Figure 4.22. Now, when a photon strikes Si, if it is of sufficient energy (about 1.1 eV or more), then it may excite an electron, freeing it from the valence band (the electron is then said to enter the conduction band) and allowing it to travel freely (and randomly) through the lattice. This leaves behind a positively charged “hole,” i.e. an unpaired

valence electron. Like the free electron, as electrons un-pair and re-pair, the hole can also migrate randomly through the lattice. This is an example of the photoelectric effect, but with a pure Si lattice, light does nothing more than create electron-hole pairs that diffuse randomly until recombining, generating no useful current, as also shown in Figure 4.22.

To utilize the photoelectric effect, we must force excited electrons to flow in a preferential direction (and hence generate current), a task accomplished through the introduction of impurities, or “dopants,” into our crystal lattice. There are two basic dopant classes: (1) n-type, which adds un-paired electrons to the lattice, and (2) p-type, which creates holes in the lattice. If we stack n-doped silicon on p-doped silicon, un-paired electrons from the n-side fill holes on the p-side, and thus the n-side develops a permanent net positive charge (as it has lost electrons), while the p-side becomes negative. It follows that shining light on such a p-n junction will generate excited electrons that flow unidirectionally to the positively charged n-type silicon. We then place wires on the silicon surface to collect up electrons, connect to an external load, and back to the p-type silicon, and thus electrons are driven in a closed loop, generating electrical current. This process, using phosphorus and boron as dopants, is outlined in Figure 4.23.

Limits to solar cell efficiency

Under standard test conditions, the conversion efficiency for silicon-based solar cells faces a theoretical upper limit of about 32% (the limit is 34% for any p-n solar cell), known as the Shockley-Queisser limit, first described in detail by those authors in 1961 [175] (who initially gave 30% as an upper limit) [176], with more recent refinements by Rühle [176]. Given this, it is rather amazing that actual monocrystalline silicon solar panels have achieved up to 25% efficiency. Thus, commercial efficiencies on the order of 15–20% are actually quite good, and further increases in efficiency are really just icing on the cake. It bears repeating: currently available photovoltaics are remarkably efficient at converting sunlight to electricity, and *it is completely unnecessary to wait for further gains before widespread commercial deployment*.

Fundamental limits. Now, a quick look at the theoretical underpinning of this 32% limit. For p-n solar cells, light energy is lost via three fundamental mechanisms: spectrum losses, radiative recombination, and current impedance. Spectrum losses are the dominant factor. To excite a valence electron to the conduction band requires a specific amount of energy, known as the *band gap energy*, E_g , which is about 1.1 eV for silicon [183]. Now, individual photons have a fixed amount of energy determined solely by the wavelength (or frequency) of light, given as

$$E_{\text{photon}} = \frac{hc}{\lambda}, \quad (4.14)$$

where h is the Planck constant, c is the speed of light, and λ is the wavelength of light, and photons of energy less than 1.1 eV are unable to induce photoexcitation. Thus, longwave infrared solar radiation is lost. Furthermore, since it requires 1.1 eV and *only* 1.1 eV to generate an electron-hole pair, any photon energy above the band gap is wasted as heat. Given the spectrum of light hitting the Earth’s surface (at solar noon), we can determine that only about 50% of the Sun’s energy can be converted into electron-hole pairs, as demonstrated schematically in Figure 4.24; silicon’s E_g of 1.1 eV is actually quite close to the optimum.

Radiative recombination is the spontaneous filling of holes by electrons (this releases energy as a photon, essentially the inverse of photoexcitation and the basis for LEDs), and some fraction of our electron-hole pairs will inevitably be lost to this process before they can generate a useful current. For silicon, about 25% of light energy is lost this way. Finally, we lose about 14% of energy to circuit resistance [175, 176]. In total, then, the fraction of light energy converted to electrical current is $50\% \times 75\% \times 86\% = 32\%$.

Silicon (Si) Lattice and Photoelectric Effect

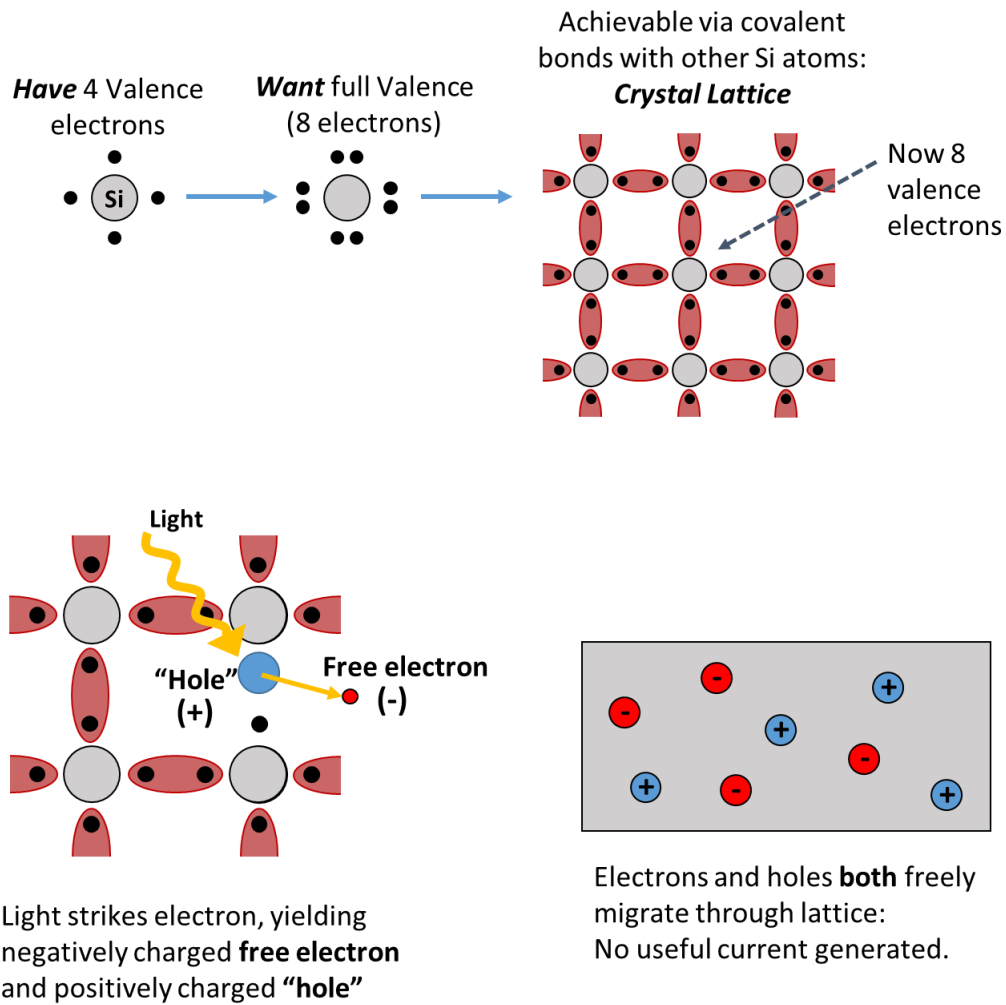
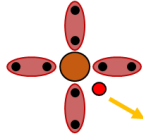


Figure 4.22: Silicon (Si) has four valence electrons, while a full valence consists of eight. Thus, electrons from four Si atoms can join pairs (covalent bonds), yielding a tetrahedral lattice (a 3-D structure but shown schematically in 2-D). Sufficiently energetic light excites electrons to yield a free electron and hole, which migrate randomly until recombining.

Dopants and the p-n Junction

n-type Dopant

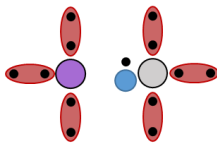
Phosphorus (P) has 5 valence electrons



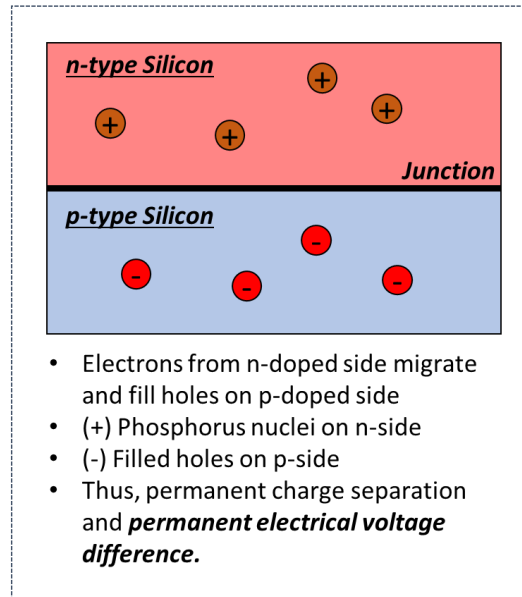
Thus, unpaired electron when in lattice → freed easily
Leaves:
(+) nucleus, (-) free electron

p-type Dopant

Boron (B) has 3 valence electrons



Thus, creates (electrically neutral) hole when in lattice



Silicon Solar Cell

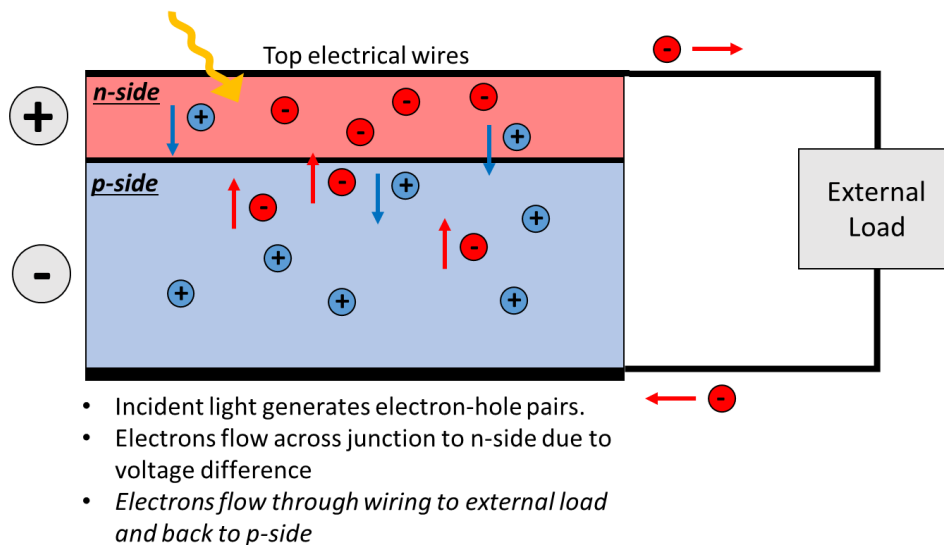


Figure 4.23: As shown in the top, n-doping of silicon entails adding phosphorus (P), which has five valence electrons. Within the Si lattice, P impurities yield unpaired electrons which readily dissociate from their nucleus. Conversely, p-doping with the addition of boron (B), which has only three valence electrons, leaves holes in the Si lattice. Upon sandwiching a layer of n-type and p-type silicon, free electrons from the n-layer fill the the p-layer holes, leaving excess positive charges in the n-doped silicon, and thus we set up a permanent charge separation and voltage drop across the p-n junction. When light shines upon a p-n junction solar cell, excited electrons are driven across the p-n junction to the n-side by the voltage difference, and then may pass through wiring across an external load and back to the p-side. Thus, an electrical current is generated.

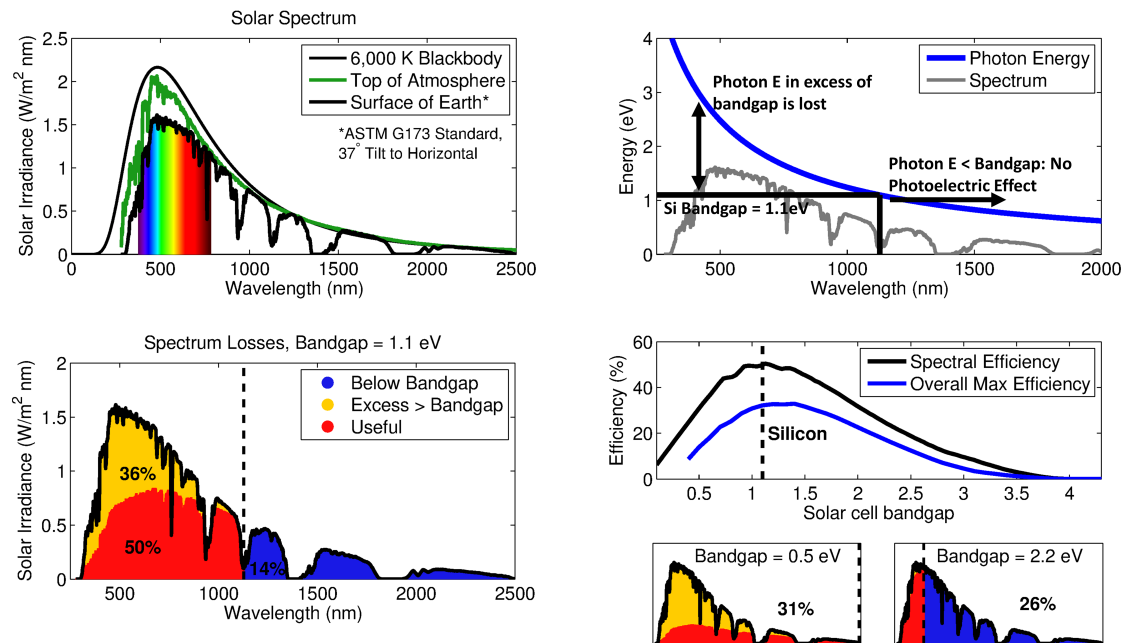


Figure 4.24: Schematic for spectral losses in a solar cell based on a single p-n junction. Photons with a long wavelength and photon energy below the bandgap, which is 1.1 eV for Si, are unable to induce photoexcitation and thus their energy is lost, while any photon energy in excess of the bandgap is also lost, leaving only about 50% useful energy across the solar spectrum when the bandgap is 1.1 eV (spectral efficiency). On the right we see how maximum spectral and actual efficiency vary with the bandgap, and spectral efficiency under two example alternative bandgaps, 0.5 and 2.2 eV, is also demonstrated (under which only 31% and 26% of light energy is useful, respectively).

Other efficiency losses. In practice, several other mechanisms also limit efficiency. Untreated silicon reflects 36% of incident light, but coating and texturing can reduce reflection losses to nearly zero. Electrical wires overlying the solar cell (necessary to collect electrons) “self-shade,” blocking a small fraction of sunlight. High temperatures also degrade solar cell performance by increasing lattice energy and interfering with the movement of charge carriers [183].

4.13.3 Emissions factors and energy pay-back time

The fabrication of crystalline silicon(c-Si) PV modules is an energy-intensive process, requiring on the order of 1,000–1,500 kWh/m² of panel area of *primary* energy. About 75% of energy used is electrical, where each kWh(e) corresponds to about 3 kWh of primary energy, and monocrystalline-silicon (mo-Si) modules require perhaps 15–35% more energy than polycrystalline-silicon (Si) to fabricate [177]. Energy payback times for silicon panels are reported to be on the order of 1.5 to 3 years [177]. For example, an array exposed to 1800 kWh/m²/yr with 15% efficiency and a 75% performance factor generates 202.5 kWh(e)/yr, which is roughly equivalent to 550 kWh of primary fossil energy (assuming 37% generating efficiency), and yielding energy payback after about two years.

The upstream emissions from solar module fabrication translate into roughly 40–50 kgCO₂e/kWh amortized over a 30-year system lifetime for c-Si-based technologies [177, 178], while thin-film technologies are probably slightly cleaner, at around 20–30 kgCO₂e/kWh [179, 177]. While some earlier (1990s) analyses suggested much higher GHG emissions associated with solar PV, marked reductions in silicon requirements, lower energy silicon processing, recycling technology, and increasing panel efficiency since then have significantly improved solar PV’s environmental profile (as reviewed by Fthenakis and Kim [177]), and lifecycle emissions are likely to continue to fall by as much as 50%. Lifecycle emissions, being total emissions divided by lifetime energy generation, are also strongly affected by solar irradiance and hence can vary more than twofold by region, with the US, and especially the southwestern US, a relatively favorable region (this regional dependence also holds for energy payback time). I now briefly review the production process and embodied energy for c-Si panels, since these account for over 90% of solar capacity globally, omitting a detailed treatment of thin-film panels (see, e.g. [179] for an in-depth discussion), as well as novel PV technologies not currently in widespread use.

Silicon PV lifecycle emissions are nearly all generated at the fabrication phase, with purification of crystalline silicon dominant. As schematized in Figure 4.25, and discussed in detail in a moment, the fabrication process entails (1) silica (SiO₂) mining, (2) purification to metallurgical grade silicon (99% pure), (3) purification to electronic- or solar-grade silicon (99.9999% pure), (4) silicon ingots cut to thin wafers, (5) wafer doping, (6) wafer etching and texturing, (7) electrode screen printing and anti-reflective coating, and finally (8) assembly into modules. Subsequently, modules are deployed to form the basis of a full PV system, which requires additional mounting and electrical components (“balance of system” components), and is illustrated in Figure 4.26.

Silicon is the second-most abundant element in the earth’s crust, and it is commonly found as silicon dioxide (SiO₂, “silica”) in sand and gravel (“silica sand” or “quartz sand”). Mined quartz sand is purified to metallurgical grade silicon (MG-Si, about 98–99% pure silicon) via reaction with carbon in an electric arc furnace at 1,500–2,000 °C [180], consuming about 12 kWh/kg MG-Si [182]:



Now, for a solar cell p-n semiconductor we require a silicon crystal lattice pure to one part

in one million (solar grade silicon, SG-Si), while for electronics the lattice must be pure to one part in a billion (electronics grade silicon, EG-Si). Either is achieved by processing MG-Si in a Siemens reactor, whereby silicon metal is volatilized via reaction with hydrochloric acid (HCl) into trichlorosilane (SiHCl_3 , TCS) gas, which is then purified by distillation. In the traditional Siemens process, TCS is converted to extremely pure Si metal via chemical vapor deposition onto a U-shaped silicon filament electrically heated to about 1,100 °C; this yields electronics-grade silicon [182].

A modified Siemens process can be used instead to produce SG-Si of lower purity. Trichlorosilane is converted to silane (SiH_4) via a series of reactions, and silane then deposits upon the seed silicon filament at 850 °C, representing a significant energy savings. This purification step, either via the Siemens or modified Siemens process, yields a large polycrystalline rod, and represents the largest use of energy in the solar production, with the Siemens process consuming on the order of 100 kWh/kg EG-Si [182]. An alternative technology, the fluidized bed reactor (FBR), uses only 10–30% the energy, but currently has only about a 10% market share.

Next, the polycrystalline rod is melted down and faces one of two fates. For polycrystalline solar cells, it is cast into a mold and then cut into 15.6×15.6 cm wafers. Alternatively, monocrystalline silicon can be produced by the *Czochralski process*, in which a seed crystal is dipped into our molten silicon and slowly withdrawn and rotated, giving a large mono-crystalline ingot, which is then cut into wafers. Wafers must then be “etched,” via a chemical bath to remove saw damage, doped with impurities (e.g. phosphorus), and the surface is randomly textured and given an anti-reflective coating to reduce reflectance from 35% to < 5% [183]. A silver electrode screen is applied to the cell’s surface, and production is complete. Each cell produces about 0.5 V, so typically 60 or 72 cells are wired together to produce a single module.

Balance of system (BOS) components account for around one-third of the overall energy and carbon footprint of solar PV, with Fthenakis and Kim giving 15 gCO₂e/kWh attributable to BOS [177]. These components include aluminum frames, mounting systems, electrical wiring, and inverters for converting the DC power produced by solar cells to AC.

I add 50 gCO₂e/kWh to all solar capacity for eGRID corrections, although given how little power is solar-generated on the national scale, this has no appreciable effect on electricity EFs.

4.14 Limits to renewable energy and energy transition

The public conversation around renewable energy is rife with controversy, and very frequent assertions to the effect that (1) renewable energy is not scalable, (2) it is too intermittent, and (3) it is too expensive. Solar energy, in particular, as a highly (but predictably) intermittent source that lends itself to distributed generation is subject to competing claims. Let us examine these objections in some detail, with the goal, as always, not to prove one side right or wrong, but to understand the issues with a clear mind. Note that in this discussion, I generally exclude biomass, the scalability of which is addressed in Section 3.8. Furthermore, it is important to remember that while most public conversation in the US centers around electricity generation, this accounts for only about 40% of primary energy use, and decarbonizing heating and transportation fuels is a further challenge. In general, I conclude that renewable resources, especially wind and solar, *are* sufficient to provide all electricity and all energy in general, from a basic resource and materials standpoint, from a cultural (i.e. grid integration) standpoint, and from a financial perspective. Nuclear is an “honorary” renewable technology that can, at least in principle, also play a role in a low carbon energy future.

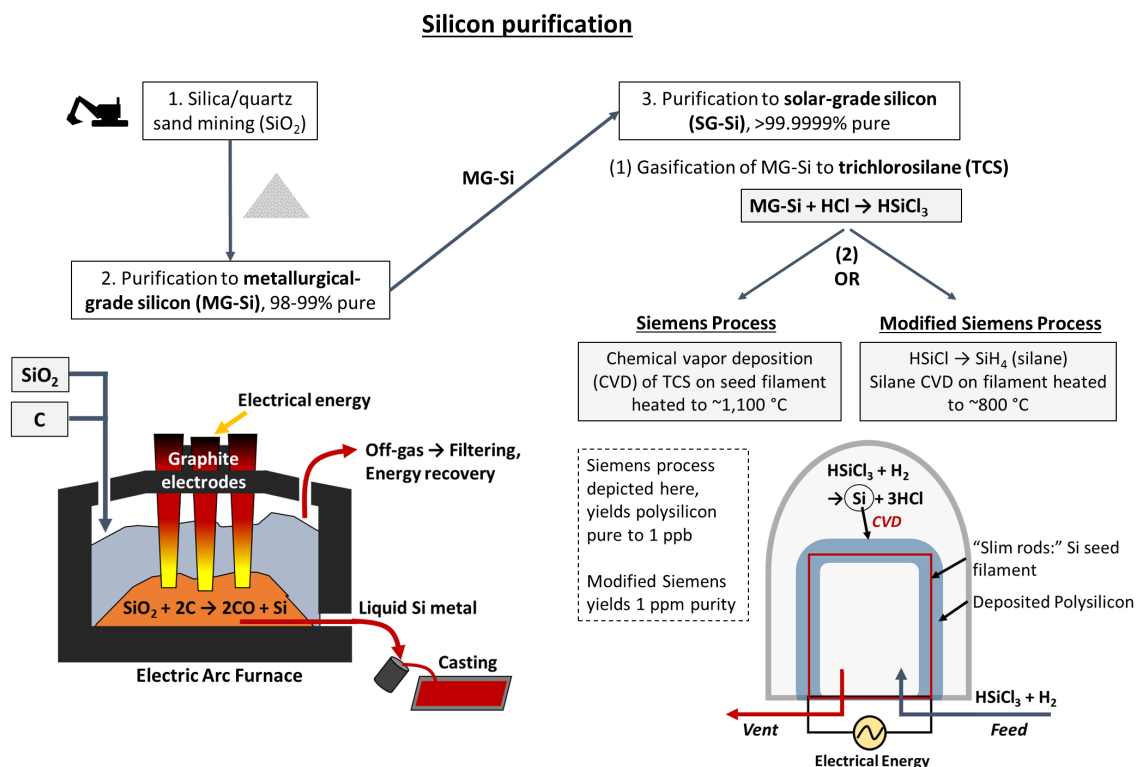


Figure 4.25: Schematic for the process of purifying quartz sand to solar- or electronics grade silicon. First, raw mined silica feedstock is fed, along with carbon, to an electric arc furnace, to yield 98–99% pure metallurgical-grade silicon (MG-Si). Much higher purity is then achieved at the major energy-consuming stage, by which either the Siemens or modified Siemens process, volatilized Si is heated and deposits upon a seed silicon filament.

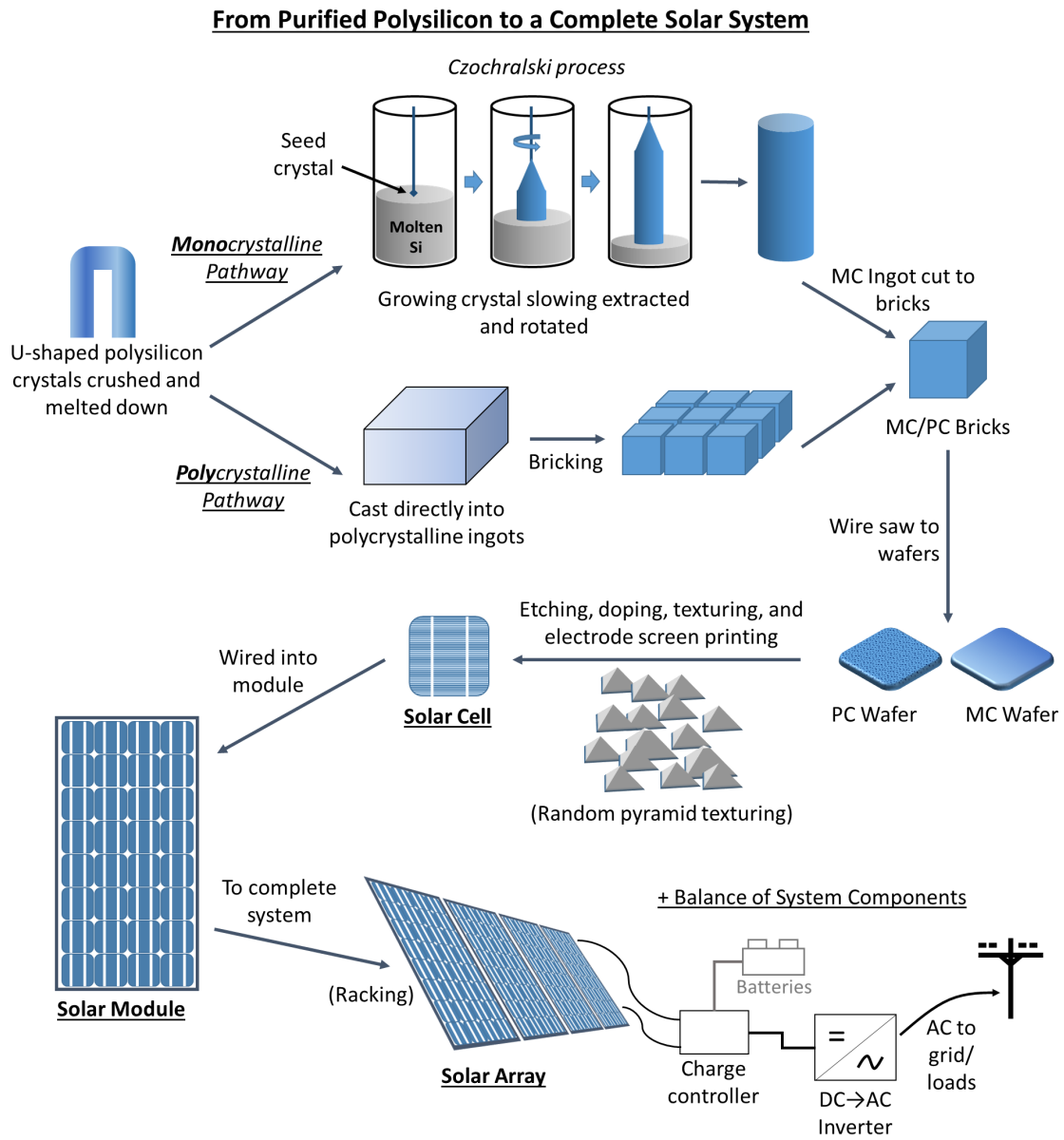


Figure 4.26: Schematic for solar cell fabrication from a polycrystalline ingot, and then incorporation into a deployed solar system.

4.14.1 Fundamental resource, land, and material limits to scaling up of renewables

- Global geophysical resources, land, and materials are all sufficient to power the world entirely with wind and solar. This also holds at the US national scale.
- The global land base is sufficient to provide all of earth's *electricity*, but possibly not all *energy*, from wind alone at plausible levels of deployment (1.5–2.0% of global land).
- Material demand, mainly steel and concrete, is not a significant constraint to large-scale wind power. Rare earth element supplies may limit the expansion of turbines that use permanent magnet generators, but these are a minority of all turbines.
- About 0.5% of global land could supply all earth's energy (including electricity) from solar PV. Solarizing about one-third of US rooftop area could provide all the nation's electricity.
- Metal availability limits thin-film PV technologies, but is unlikely to constrain crystalline-silicon PV (the dominant technology).

Intermittency, demand-supply balancing, incorporation into existing energy transportation and distribution networks, etc. are at least partly cultural, rather than technological, limits to renewable energy. The physical availability of energy resources, and the land-base and materials required to extract them (under existing technologies) represent more fundamental limits. Fortunately, as we shall see, all of these are sufficient for a world powered entirely with wind and solar.

Fundamental limits to wind

Geophysically, Marvel et al. [173] concluded that harvestable near-surface wind resources amount to over 400 TW, equal to about 3.75 trillion MWh/yr, or around 24 times global primary energy consumption and 174 times global electricity generation. However, this calculation assumes uniform harvesting across the entire globe, both land and sea, and the real question is, how much could feasibly be extracted?

Only 14.894 billion Ha out of 51.007 billion Ha of global area is land (CIA World Fact Book), and perhaps 13% of land experiences average wind speeds ≥ 6.9 m/s at 80 m [184], where wind harvesting is relatively economical. Turbines extract kinetic energy from the air, with the result that large-scale wind harvesting is clearly limited to around $1 \text{ W(e)}/\text{m}^2$ [186, 159], and therefore such a land-base could yield about 170 billion MWh, roughly eight times global electricity generation and just over global primary energy consumption. It follows that wind energy could, in principle, supply most or all electricity using only a fraction of the suitable land area, around 1.5–2.0% of the globe's land, but providing *all* energy from wind is a less likely proposition.

Note that several published estimates, e.g. [184, 185], by ignoring the limiting effect of large-scale turbine deployment on wind energy extraction (turbines sap the air of kinetic energy), have likely significantly overstated feasible wind resources severalfold, as elaborated by Adams and Keith [186]. For example, an estimate by Archer and Jacobson [184] of 72 TW extractable from the 13% of land with economically sufficient wind speeds corresponded to a power density of $4.3 \text{ W}/\text{m}^2$: too high by a factor of four.

Wind turbines require large amounts of steel, concrete, fiberglass and epoxy for the tower, foundation, and blades, respectively, but supply of these materials is not likely to be a major barrier to large-scale wind harvesting [188]. The rare earth elements (REEs) neodymium (Nd) and dysprosium (Dy) are components of permanent magnet electric generators used in gearless

direct-drive wind turbines, which were introduced in 2003, and reached a 14% market share by 2007 [190] (induction generators, used in the majority of turbines, do not require REEs [191]). Because exploitable reserves of these elements are rather scarce, and nearly all REEs are mined and produced in China, which recently instituted export quotas, they represent a potential material limitation to upscaling of *direct-drive* wind power and, far more importantly, motors for electric vehicles [190]; several authors have examined REEs as limiting factors for renewable energy technologies, e.g. [189, 190].

In 2010, wind turbines accounted for only 1% of Nd and Dy use, and were projected by Habib and Wenzel [190] to remain a minor end-use in 2050 under multiple energy scenarios, including a 100% renewable energy scenario (electric vehicles were the dominant user in this case). Therefore, high REE demand due to background uses (e.g. consumer electronics) and electric vehicles could limit the penetration of direct-drive turbines in the future, but REEs are *not* a material constraint on wind power in general.

Limits to solar

- Geophysical resources and the land base do not limit solar; existing urban rooftops are more than sufficient to provide all global electricity.
- Metal availability strongly limits some thin-film PV technology (CdTe, CIGS), but silicon reserves are vast.
- Silver (used for electrodes) is the only significant material limitation to very large-scale (terawatt) crystalline silicon PV, but PV silver content is falling rapidly, and copper is a viable replacement metal.

Geophysical solar resources vastly exceed civilization's energy consumption. Jacobson [187] reports 1,700 TW of solar PV potential over the globe's land, corresponding to nearly 100 times global primary energy demand. The continental US alone (766 billion Ha in area, about 5% of earth's land), assuming an average solar insolation of 1,800 kWh/yr, energy conversion efficiency of 15%, and a performance factor of 75%, could in principle supply about ten times the global primary energy demand. It follows that, using reasonably well-sited solar PV, about 0.5% of earth's land could supply all global energy (supplying all electricity would require a miniscule 0.07% of global land); even in energy-hungry America, just 0.27% of the continental US could supply all the nation's electricity. Note that urban rooftop area is likely sufficiently large to meet all solar land requirements, and thus, if distributed solar is seriously pursued, few new lands need be devoted to solar farming (see calculations in Section 4.14.2 below).

Existing metal reserves and extraction rates *strongly* limit the scalability of CdTe and CIGS thin-film PV panels (currently <10% of PV), and these technologies can never provide more than a few percentage points of the world's electricity [192]. Crystalline silicon-based PV, on the other hand, is not limited by silicon availability: silicon reserves are vast, and 100% of global electricity could be supplied by c-Si PV in 2030 without Si production growth exceeding historical growth rates [192].

Silver (Ag), which is screen-printed onto panels to form the top electrodes in c-Si cells, does potentially limit the deployment of silicon PV at terawatt scales [193]: it would take on the order of 50–100% of existing silver reserves (about 570 kilotonnes [195]) to provide all global electricity with c-Si PV at current use rates, which were reported to be about 4 g Ag/m² in 2015 by [196], a marked reduction from even a few years earlier (some slightly earlier estimates are 57 mg Ag/W in [192] or 8.2 g Ag/m² [194]). Silver is also used at lower rates in concentrating solar power (CSP) as a highly reflective mirror coating, at about 1 g Ag/m² (CSP achieves

electrical conversion efficiencies in the 15–20% range, similar to PV) [194].

In general, silver is a major limiting material for industrial civilization, as it is widely used in electronics (silver has the highest electrical conductivity of any metal), photography (silver halides are light-sensitive, but are being replaced by digital photography), and other industrial applications; jewelery is the other major use of silver, recently demoted to second place after electronics. Rather remarkably, about 75% of all silver reserves have already been mined (with ongoing mining since at least 4,000 B.C.E.), and at current mining rates (27,300 tonnes/year in 2015 [195]), all reserves will be exhausted in only two decades; nearly all silver must come from recycled sources in the very near future. One may consult Grandell and Thorenz [194] for further discussion of the silver cycle and implications for solar technology.

Despite the rapidly approaching “peak silver,” this metal is unlikely to ultimately limit solar PV (or CSP) [192], as its use in c-Si PV is projected to fall by over half from 2015 to 2026 [196], and copper will probably eventually displace silver, with silver PV content falling by an order of magnitude. Copper is a viable replacement metal that has been used in several commercial (but sadly now defunct) panels: “Saturn” panels by BP-solar, “Pluto” panels by Suntech, and, most recently, highly efficient TetraSun panels employing copper electrodes were briefly produced by First Solar until discontinuation in the summer of 2016. Concentrated solar power uses silver at a low rate compared to PV, and aluminum is an alternative mirror coating if needed.

4.14.2 Is rooftop solar scalable? Some back of the envelope calculations

- Solarizing roughly one-third of the US’s urban rooftop area (0.27% of total continental US land area) could, in principle, supply all US electricity. Concentrating generation in the South and Southwest would reduce this fraction.

Total US electricity generation in 2010 was 4,125.847 billion kWh (eGRID), and therefore, using the US average irradiance of 1,800 kWh/m²/yr, module efficiency of 15%, and a performance ratio of 0.75, it would take about 7,900 square miles of PV panels to replace all 2010 generation. The fraction of urban area that is rooftop is 20–25% [197]; assuming 20% roof area, we would then require 39,333 square miles of urban area, with every single rooftop completely covered by PV panels.

Total urban area in the US is, as of the 2010 Census, 106,000 square miles. Thus, solarizing 37% of US urban rooftop area (conservatively assuming 20% of urban area is rooftop) could theoretically meet the entire US electricity demand (only 27% of rooftop area would be needed if average module efficiency increased to 20%). Consider as a local example the case of California, which generated 204 billion kWh in 2010. Under the higher southwest irradiance of 2,400 kWh/m²/yr, the entire state’s demand could be met if 84% of rooftop area in the Los Angeles/Long Beach/Anaheim urban area (1,736 square miles total) was solarized.

4.14.3 Some notes on renewable variability and grid integration

The variability of wind and solar energy resources is a barrier to adoption, but one that does appear to be insurmountable (and even if it is, there is no alternative to an eventual fossil-free future). Several studies have concluded that using existing technologies, wind and solar, along with nuclear and large hydropower, can provide essentially 100% of electricity (and potentially all heat and transportation energy as well) at US regional, US national, various European country, continental, and global scales on a decadal timescale, at modest cost or even net savings compared to fossil-based generation [198, 199]. That does not mean that this will happen, but

it does mean that the challenge facing an energy transition is primarily one of political will, and not one of technological (or even economic) constraints.

Briefly, to understand the challenge wind and solar represent, regional electricity grids classically operate on under a dispatch model, where to match electricity supply with demand, we have a hierarchy of generating plants—baseload, load-following, and peaking—that are *dispatched* as the load on the grid increases. At the bottom, baseload generating plants, classically coal-fired or nuclear steam plants, operate near full capacity at nearly all times (excepting scheduled maintenance). Combined cycle natural gas (CCNG) plants also generally operate as baseload generators, but have some ability to load-follow, as do some nuclear plants. Load-following plants are intermediate and may ramp up or down to meet demand. Other natural gas turbines may operate either as load-following plants or peaker plants. Economically, there is a clear relationship between resource type and generating costs, with baseload generation cheapest, and peak resources by far most expensive, and hence the economic incentive to avoid energy use at peak hours.

To cope with regularly fluctuating demand that does not coincide with fluctuating and sometimes erratic generation, the so-called *supply-demand balancing* problem, a *local* renewable electricity system (disregarding flexible hydropower generation) will generally require either supplemental fossil-fuel generation and backup, or significant energy storage capacity (or both). Even under such a model of localized renewable generation, intermittent renewables can significantly displace fossil generation, with several European countries already generating around 20% of their power portfolios with wind and solar. While wind and solar may vary unpredictably at local scales, at the large regional scale variability smooths out, and with regional grid interconnections most US electricity demand could, in principle, be met purely by wind, water and solar, *without* energy storage or significant fossil backup using the *current* electrical grid [198]. In a future system, complete energy system electrification in combination with thermal energy and hydrogen storage could also meet 100% of global demand without any fixed battery storage [200]. A well-designed near-term regional system could still likely provide 33–50% of power with primarily wind and solar renewables with little over-generation [201], and one study concluded, for example, that Germany could generate up to 50% of its electricity with wind and solar without any energy storage [202]. In sum, renewable integration is a genuine but not intractable technical challenge, and this should highlight the value of energy conservation, which can both reduce the total amount of fossil energy that must be replaced, and synergize with renewable generation to decrease carbon emissions.